Published in final edited form as:
Exp Neurol. 2013 March ; 241: 125–137. doi:10.1016/j.expneurol.2012.12.010.

Anterograde trafficking of neurotrophin-3 in the adult olfactory system in vivo

Huan Liu, **Michael Lu**, and **Kathleen M. Guthrie***
Department of Basic Biomedical Science College of Medicine Florida Atlantic University Boca Raton, FL, 33431

Abstract

The olfactory system continuously incorporates new neurons into functional circuits throughout life. Axons from olfactory sensory neurons (OSNs) in the nasal cavity synapse on mitral, tufted and periglomerular (PG) cells in the main olfactory bulb, and low levels of turnover within the OSN population results in ingrowth of new axons under normal physiological conditions. Subpopulations of bulb interneurons are continually eliminated by apoptosis, and are replaced by new neurons derived from progenitors in the adult forebrain subventricular zone. Integration of new neurons, including PG cells that are contacted by sensory axons, leads to ongoing reorganization of adult olfactory bulb circuits. The mechanisms regulating this adaptive structural plasticity are not all known, but the process is reminiscent of early nervous system development. Neurotrophic factors have well-established roles in controlling neuronal survival and connectivity during development, leading to speculation that trophic interactions between OSNs and their target bulb neurons may mediate some of these same processes in adults. A number of different trophic factors and their cognate receptors are expressed in the adult olfactory pathway. Neurotrophin-3 (NT3) is among these, as reflected by beta-galactosidase expression in transgenic reporter mice expressing lacZ under the NT3 promoter. Using a combination of approaches, including immunocytochemistry, real-time PCR of laser-captured RNA, and adenovirus-mediated gene transfer of NT3 fusion peptides in vivo, we demonstrate that OSNs express and anterogradely transport NT3 to the olfactory bulb. We additionally observe that in mice treated with adenovirus encoding NT3 tagged with hemagglutinin (HA), a subset of bulb neurons expressing the TrkC neurotrophin receptor are immunoreactive for HA, suggesting their acquisition of the fusion peptide from infected sensory neurons. Our results therefore provide evidence that OSNs may serve as an afferent source of trophic signals for the adult mouse olfactory bulb.

Introduction

The adult olfactory system is unique in its ability to incorporate new neurons throughout life, both peripherally in the nasal cavity, and centrally in the olfactory bulb. New olfactory sensory neurons (OSNs) are generated from resident basal stem cells in the olfactory epithelium (OE), a process that allows for slow replacement of mature sensory neurons as those subjected to normal environmental damage over time (due to their vulnerable location

*Corresponding author: Kathleen Guthrie, Ph.D. Dept. of Basic Biomedical Science, BC 208 Charles E. Schmidt College of Medicine Florida Atlantic University 777 Glades Road, Boca Raton, FL, 33431 Phone: 561-297-0457, FAX: 561-297-2221 kguthrie@fau.edu.

Supplemental material: None

Conflict of interest statement: The authors declare no conflict of interest, financial or otherwise.

in the nasal cavity) are lost via apoptosis (Magrassi and Graziadei, 1995; Mahalik, 1996; Deckner et al., 1997; Carter and Roskams, 2002; Kondo et al., 2010). New olfactory bulb granule and periglomerular (PG) neurons are continuously generated from progenitors in the adult forebrain subventricular zone (SVZ; Nissant and Pallotto, 2011). A portion of these new interneuron populations survive and functionally incorporate into bulbar circuits, as subsets of previously established bulb neurons gradually undergo apoptosis, a process that is controlled in part by an animal's olfactory environment (Petreanu and Alvarez-Buylla, 2002; Lledo and Saghatelyan, 2005; Mandarion et al., 2006; Imayoshi et al., 2009; Mouret et al. 2009). OSN axons synapse on the dendrites of bulb mitral, tufted and type 1 PG cells, and adult-born PG cells establish functional connections with these axons as they integrate into the olfactory bulb's glomerular layer (Kosaka and Kosaka, 2005; Grubb et al., 2008). As a result of this considerable anatomical plasticity, the adult olfactory pathway maintains many features characteristic of developing neural systems (Verhaagen et al., 1989; Nacher et al., 2001; Schwob, 2002).

Neurotrophic factors are well known as regulators of neuronal survival, differentiation, and connectivity during development (Huang and Reichardt, 2001), and trophic interactions between the olfactory bulb and its innervating sensory neurons have long been postulated (Schwob et al., 1992; Leo et al., 2000; Cowan et al., 2001; Ferrari et al., 2003; Hayward et al., 2004; Ardiles et al., 2007). A wide variety of identified factors and their cognate receptors have been localized to the olfactory system (Mackay-Sim and Chuah, 2000; Schwob, 2002; Langenhan et al., 2005). These include the nerve growth factor (NGF) family of neurotrophins and their tropomyosin receptor kinase (Trk) receptors (Guthrie and Gall, 1991; Deckner et al., 1993; Carter and Roskams, 2002). Neurotrophins function as target-derived, retrograde survival factors for populations of developing peripheral neurons, but are also important mediators of dendritic maturation and maintenance, as well as synaptic plasticity, in the central nervous system (CNS), actions that are not limited to development (McAllister et al., 1996, 1999; Gorski et al., 2003; Lu, 2004; Conner et al., 2009; Rauskolb et al., 2010). In some instances, these signals are provided via anterograde transport, with innervating axons supplying endogenous neurotrophins to postsynaptic CNS targets (Conner et al., 1997). Examples include the anterograde transport of brain-derived neurotrophic factor (BDNF) by corticostriatal afferents and of neurotrophin-3 (NT3) and BDNF by developing optic nerve projections (von Bartheld and Butowt, 2000; Caleo et al., 2000; Baquet et al., 2004).

NT3 expression has been indirectly localized to OSNs in heterozygous reporter mice in which most of the NT3 coding sequence is replaced by the *E. coli* lacZ sequence under control of the NT3 promoter (Farinas et al., 1994; Vigers et al., 2003). Bulb neurons that receive input from OSNs express TrkC, the preferred NT3 receptor (Deckner et al., 1993), suggesting that like the developing visual system, the olfactory pathway may utilize NT3 as an anterograde trophic signal. Here we use a combination of immunocytochemistry, semi-quantitative, real-time (Q-RT) PCR of laser-captured RNA, and viral-mediated gene transfer of NT3 fusion peptides, to show that OSNs express and anterogradely transport epitope-tagged NT3 to their target, the adult olfactory bulb, in vivo.

Material and Methods

Laser Capture Microdissection and RNA isolation

All animal procedures were approved by the Florida Atlantic University Institutional Animal Care and Use Committee and adhered to National Institutes of Health guidelines. Six adult female C57Bl6 mice (19-23 g, 8-12 wks, Charles River Laboratories, Raleigh, NC) were euthanized with sodium pentobarbital (150 mg/kg, i.p.) and decapitated. Nasal cavities were dissected, embedded in OCT medium and frozen in isopentane (-50°C). The hippocampus

was dissected and frozen on dry ice. Coronal cryosections (8 μm) through the nasal cavities/olfactory epithelium were collected on LCM membrane slides (Arcturus, Applied Biosystems, Carlsbad, CA) and stored at -80°C. Additional sections were cut and dropped intact into extraction buffer for RNA purification (Arcturus PicoPure RNA isolation kit). Immediately prior to laser capture, slides were removed from storage, fixed in 75% ethanol (-20°C), then stained and dehydrated through increasing concentrations of ethanol using the Arcturus Histogene staining kit according to instructions. Final dehydration was carried out in 100% ethanol for 2 min followed by 6 min in xylene. Olfactory epithelium was visualized and samples captured at 20-40X objective magnification using the ArcturusXT Laser Microdissection instrument. In NT3-lacZ mice, OSN beta-galactosidase expression is detected throughout the OE, with particularly high levels seen in posterior endoturbinates (Vigers et al., 2003). In order to obtain sufficient amounts of material for RNA isolation, our samples were captured throughout the OE, and were not limited to particular locations. UV laser cuts were used to separate and lift a region containing olfactory sensory neurons (OSNs) located in the middle depth of the epithelium, to avoid collecting progenitor cells situated more deeply, and sustentacular cells located superficially. When necessary, UV-cut samples were pulsed with the IR laser (16-20 msec, 20μm spot size, 65-72 mW) to facilitate attachment to Arcturus HS LCM collection caps (Fig. 1A). Samples lifted from 2-3 coronal sections were collected on each cap. Collection membranes were removed from caps, placed in 50 μl of RNA extraction buffer (Arcturus), and incubated at 42°C for 30 min. Membranes were removed and samples were stored in extraction buffer at -80°C prior to isolation of total RNA using the Arcturus PicoPure procedure with DNase treatment according to kit instructions. RNA from dissected hippocampus was isolated using Qiagen's RNeasy Plus kit (Qiagen, Valencia, CA). RNA concentration and quality was assessed by Qubit assay (Invitrogen, Carlsbad, CA), and by Pico Chip assay (Agilent Technologies, Santa Clara, CA) using the Agilent 2100 Bioanalyzer. The resulting electropherograms were examined and samples with RNA integrity numbers (RIN) lower than 6.0 were excluded from further analysis.

Semi-Quantitative RT-PCR

RNA samples were reversed transcribed and PCR-amplified using Stratagene's Brilliant II One-step RT-PCR kit (Agilent). FAM-labeled Taqman probe/primer assays from Applied Biosystems were used to amplify mouse NT3 (#Mm01182924_m1), BDNF (#Mm01334042_m1), NGF (#Mm00443039_m1), NT4 (#Mm01701591_m1), and olfactory marker protein (OMP, #Mm00448081_s1). VIC-labeled mouse beta-actin assays (#4352341E) were used for normalization. Amplification standard curves were first generated for all sequences using serial dilutions of RNA isolated from intact cryostat sections through the nasal cavities/OE (15-240ng per reaction). Amplification efficiencies for all neurotrophins ranged from 95-108% and r^2 values ranged from 0.984-0.998. Reactions using laser-captured OSN samples were performed in triplicate using 45ng of total RNA pooled from all OE samples, random primers, the specific Taqman probes, and Stratagene's MxPro3000P Q-PCR instrument. Parametric studies have shown that tissue treatment procedures for laser capture microdissection (fixation, staining, laser pulsing, collection duration) tend to reduce RNA quality when compared to RNA isolated from fresh, non-laser captured tissue samples (Kerman et al., 2006). Recommended parameters for RT-PCR using total RNA isolated by laser capture microdissection include amplified product lengths of 200 bases or less, and RNA integrity numbers (RIN) greater than 5 (Fleige et al., 2006; Erickson et al., 2009). We discarded all samples with RIN values below 6, and our amplicon sizes ranged from 69-110 bases. The final RIN of our pooled, laser-captured OSN RNA was 6.5. As expected, the RIN for RNA isolated from non-laser captured hippocampal samples was higher (8.5). Reverse transcription reactions were carried out at 42°C for 1 hr, followed by 10 min denaturing at 95°C, and 40 cycles of

amplification (95°C-15 sec, 60°C-1 min). Reactions using Taqman OMP primers were included to verify collection of RNA from OSNs, and reactions using total RNA from hippocampus (20ng) were included as positive controls for detection of neurotrophin transcripts. Each triplicate assay was performed twice, for a total of 6 measurements per transcript, and template RNA was omitted from control assays. MxPro3000P software was used to normalize neurotrophin values (delta Ct) relative to the mean Ct of beta-actin. BDNF and NT3 transcript abundance in the OE were both calibrated and graphed relative to NGF (mean set to 1.0), also using MxPro3000P software. NT4/5 expression was not detectable in either the OE or hippocampus.

Antibody production and NT3 immunolocalization

Three synthetic peptides corresponding to regions within mature mouse NT3 having the least homology to BDNF and NGF were used as antigens in combination to generate a rabbit polyclonal antibody, with the same three peptides used for final affinity purification of the IgG fraction isolated from serum (ProteinTech Group Inc, Chicago, IL). The sequences were as follows: CLGEIKTGNSPVKQY, TSENNKLVGWRWIC, CVTDKSSAIDIRGHQ. Each peptide was coupled to keyhole limpet hemocyanin prior to in vivo administration to a New Zealand white rabbit. The specificity of the final antibody was verified by Western blot detection of human recombinant (hr)NT3 peptide, with hrBDNF, hrNT4 and mouse NGF (all mature peptides, ~13-15kDa) used as controls (Peprotech Inc., Rocky Hill, NJ). Samples of purified peptide (1μg) were subjected to SDS-PAGE (18%) under reducing conditions and transferred to nitrocellulose membranes. Blots were probed using the rabbit anti-NT3 antibody (1:5000) and goat HRP-labeled anti-rabbit IgG (Millipore, Temecula, CA, 1:20,000) followed by chemiluminescent detection (SuperSignal Kit, Thermo Scientific, Waltham, MA).

For immunohistochemistry, five young adult female C57Bl6 mice (19-23g, 6-8 wks of age, Charles River) were euthanized with sodium pentobarbital as above and perfused with phosphate-buffered saline (PBS, pH 7.3), followed by 2% paraformaldehyde (PFA) in 0.1 M phosphate buffer (PB) containing 0.2% parabenzoquinone (PBQ). Brains and attached nasal cavities were dissected, postfixed for 2 hrs, and transferred to 30% sucrose in PB. Tissue was embedded in 10% gelatin, which was postfixed in 2% PFA and cryoprotected with 30% sucrose, and frozen in isopentane (-50°C). Horizontal cryosections through the brain and nasal cavities (25-30 μm) were processed free-floating. Preliminary staining indicated only very faint OE labeling with immunofluorescent detection, and consequently sections were processed using immunoperoxidase methods with signal amplification (Vector Elite ABC reagent; Vector Laboratories, Burlingame, CA). Tissue was treated with 1% H_2O_2 for 10 min, and blocked in 10% BSA in PBS with 0.15% Triton-X-100 for 2 hrs. After rinsing, primary antibody incubation was performed at 4°C for 48 hrs at a dilution of 1:800 in the blocker solution. Sections were treated sequentially with biotinylated anti-rabbit IgG (Vector Laboratories) for 1.5 hrs at RT, followed by avidin-biotin-HRP complex (Vector Elite kit) for 1.5 hrs. Reaction product was developed using Vector's IMPACT DAB kit using half the chromagen concentration recommended by the manufacturer. Controls included omission of the primary antibody, incubation in pre-immune serum (1:800), and in antibody pre-absorbed overnight with hrNT3 (Peprotech; 30μg/ml). Sections were examined using an Olympus AX-70 microscope equipped with a Magnafire digital camera.

Production of recombinant adenoviruses

To monitor the synthesis and transport of NT3 in vitro and in vivo, adenovirus-mediated gene transfer of NT3 tagged with either enhanced green fluorescent protein (GFP) or hemagglutinin (HA) was employed. Adenoviruses are ideally suited to infection of OSNs, as these neurons express the Coxsackie-Adenovirus receptor (Zhao et al., 1996; Venkatraman

et al., 2005). GFP provides a bright, photostable tag which can be directly imaged, and has been widely used to characterize the sorting, packaging, localization and secretion of neurotrophins in vitro, particularly BDNF (Haubensak et al., 1998; Hartmann et al., 2001; Egan et al., 2003; Adachi et al., 2005; Brigadski et al., 2005; Kuczewski et al., 2008; Dean et al., 2009; Baj et al., 2011). A drawback is its relatively large size (238 amino acids) compared to the neurotrophin peptides themselves (~120 amino acids), and its ability to form oligomers when expressed in the secretory pathway, with the possibility of this ultimately altering their biological activity (Jain et al., 2001). Small epitope tags that are less likely to disrupt activity, such as HA (9 amino acids) and myc (10 amino acids), also have been used as labels for localizing neurotrophins in vitro, as well as in vivo (Ng et al., 2007; Yang et al., 2009). Though unlike GFP these epitopes cannot be directly imaged, they can be localized using antibodies, with the attendant caveats associated with antibody specificity and fixation sensitivity. Our NT3 fusion constructs utilized both GFP and 3xHA (27 amino acids) epitope tags.

The coding sequence of mouse prepro-NT3 (Genbank Access# NM-008742.3) was obtained from a plasmid provided by American Type Culture Collection (IMAGE clone 1177923). For the GFP-tagged construct, PCR amplification was carried out using an upstream primer that introduced a 5' Bgl II restriction site, modified the Kozak sequence (GGCGCC), and maintained the signal peptide sequence. The 3' primer incorporated a BamHI site at the C terminus while also removing the stop-codon. The resulting sequence was ligated into the pEGFPN1 vector (Clontech, Mountain View, CA), followed by cloning into Bgl II/Not1-digested pShuttle-CMV vector (AdEasy XL Adenoviral Vector kit, Stratagene/Agilent Technologies, La Jolla, CA). For the hemagglutinin (HA)-tagged construct (NT3-3xHA-IRES-GFP), amplification was carried out using the NT3-GFP sequence as template, the same 5' primer, and a 3' primer that introduced Xho1 and Cla1 sites. The resulting sequence was cloned into Bgl II/Xho1-digested pShuttle-IRES-hrGFP-2 (Stratagene, La Jolla, CA). Recombinant constructs were verified by DNA sequencing (Davis Sequencing, Davis, CA). BJ5183 bacteria pre-transformed with the pAdEasy-1 adenoviral vector (Stratagene) were transformed with linearized shuttle vectors containing GFP, NT3-GFP, or the bicistronic NT3-3xHA-IRES-GFP sequences to produce recombinant, replication-deficient adenovirus (serotype 5) according to the manufacturer's instructions. Recombinants were amplified in XL-10-Gold bacteria and AD-293 cells were transfected with the resulting recombinant DNA to produce primary viral stocks. GFP expression by infected cells was visualized microscopically. Viral stocks were amplified by three rounds of passaging in AD-293 cells, and the resulting viral particles were isolated using Stratagene's AdEasy virus purification kit, or standard cesium chloride density gradient methods. Titers were measured by overlay plaque assay of infected AD-293 cells (Takara Sea Plaque agarose), and purified viruses were stored at -80°C. Immediately prior to use, virus solution was dialyzed against sterile PBS for 1 hr using MiniDialysis membrane units (Thermo Scientific, 10K MW cut off).

Western blot analyses of fusion peptide expression in vitro

COS7 cells (ATCC) were seeded at a density of 2×10^5 cells/ml in DMEM supplemented with 10% FBS and maintained overnight. Cells were infected the next day with virus-containing supernatant (25μl/ml DMEM) collected from AD-293 cultures 48 hrs after infection with AdNT3-GFP or AdNT3-3xHA-IRES-GFP. Cells were gown for 72 hrs, then were collected and homogenized in Tris-SDS buffer to prepare lysates. Protein was determined by Qubit assay (Invitrogen), and heat-denatured samples (15 or 45μg) were subjected to 12% SDS-PAGE under reducing conditions, with hrNT3 used as a control (30-100ng mature NT3, Peprotech Inc.). Samples were transferred to nitrocellulose membranes (0.45μm), which were blocked in 5% BSA in Tris-buffered saline (TBS) with 0.1% Tween 20 for 1 hr. Primary antibodies were diluted in Li-Cor Odyssey blocking buffer

(Li-Cor Biosciences, Lincoln, NE). Incubations were carried out at 4°C overnight and employed rabbit anti-NT3 from Santa Cruz Biotech (1:1000, #sc-547, Santa Cruz, CA), or our rabbit anti-NT3 (1:250) combined with mouse anti-GFP (sc-9996; 1:1000; Santa Cruz Biotech), or mouse monoclonal anti-HA (4.5μg/ml, clone 16B12, #MMS-101R, Covance, Princeton, NJ). Control blots of lysates from NT3-3xHA infected COS cells were incubated with our rabbit NT3 antibody (1:250) preabsorbed with 3.3 μg/ml hrNT3 peptide (PeproTech). Blots then incubated in a cocktail of Li-Cor Odyssey infared dye-labeled IgGs specific for rabbit (dye 700) and mouse (dye 800). Secondary antibodies were diluted 1:10,000 in TBS, and incubation was carried out for 1 hr. Membranes were examined using the Li-Cor Odyssey Fc imaging system. Image files were exported to Adobe Photoshop CS3 for figure assembly, with adjustments made for size and brightness.

ELISA measurement of NT3 secretion in vitro

Release of NT3 by infected COS7 cells was quantified by enzyme-linked immunoassay (ELISA) using the Promega Emax NT3 Immunoassay kit (Madison, WI). COS7 cells were grown and infected with AdNT3-GFP or Ad-GFP as above. Cells were grown for 72 hrs and vesicular or cytosolic GFP expression was monitored by fluorescence microscopy. Media was collected from 2 sets of cultures per construct for ELISA assay of total NT3 (pro- and mature NT3), according to the Emax Immunoassay kit instructions, using chemiluminescence detection and triplicate samples for each set.

Immunostaining of adenovirus-infected cell cultures

Cellular localization of fusion peptides was examined in COS7 and N2a neuroblastoma cells (ATCC), infected with adenovirus as described. N2a cells develop neurites in culture, permitting localization of the tagged peptides in neuronal processes. Cells were infected with AdNT3-GFP, AdNT3-3xHA-IRES-GFP, or Ad-GFP as described. One to three days after infection, cells were fixed for 10 min in cold 4% PFA, rinsed in 0.1 M PB, permeabilized with 0.5% Triton X-100 for 10 min, and blocked with 1% normal goat serum for 20 min. Incubation in mouse anti-HA (0.8μg/ml, Covance) or rabbit anti-secretogranin II (1:500, # PA110838, Thermo Scientific) was carried out for 1 hr at 37°C, followed by incubation in AlexaFluor594-conjugated anti-mouse or anti-rabbit IgGs (1:1000; Life Technologies) for 1 hr at RT. Cells were counterstained with Vectashield containing DAPI (Vector Laboratories) and examined using a Zeiss 710 LCM confocal microscope.

Dorsal root ganglion neurite outgrowth

Dissociated neonatal rat dorsal root ganglion (DRG) neurons (Lonza Walkersville Inc., Walkersville, MD) were plated on poly-L-lysine/laminin dishes and cultured for 60 hrs (5% CO_2, 37°C) in DMEM with 10% fetal calf serum (FCS), 2% glucose, 1 mM glutamine, 10 μM Ara-C (Sigma), and 1% ampicillin. After washing with DMEM, cells were switched to the same medium as above, but containing only 1% FCS. At this time, duplicate sets of cultures were supplemented with recombinant NT3 peptide (100 ng/ml medium; Peprotech), or with conditioned medium (CM, 80μl/ml) collected from COS7 cells 3 days post-infection with either Ad-GFP or AdNT3-3xHA-IRES-GFP, and filtered with Millipore Amicon spin columns (50K MW cutoff). Peptide and CM treatments were repeated the following day, and control cultures were untreated throughout the experiment. Cells were grown for one more day and were examined and photographed under phase/Normarski optics using a Nikon TE-2000E Eclipse microscope with a Hamamatsu Orca-ER digital camera. At 50 hrs after initial CM treatment, images of 70 neurons (with at least one elaborated neurite) per culture condition were collected. Most neurons showed bipolar morphology at this time, while others displayed one primary neurite. Length of the longest neurite emerging from the soma of each cell was measured from calibrated images using a Macintosh computer and the public domain NIH Image program (developed at the U.S. National Institutes of Health and

available on the Internet at http://rsb.info.nih.gov/nih-image/). Mean neurite length for each treatment group (+/-SEM) was calculated, with one-way ANOVA used to test for significant effects, followed by Bonferroni's multiple post-hoc comparisons. Cultures were returned to incubation for 2 more days, and representative surviving neurons were photographed to illustrate morphology.

Viral infection of olfactory sensory neurons in vivo

Adult female C57Bl6 mice (Charles River) were anesthetized with ketamine-xylazine cocktail (0.08 mg/g and 0.012 mg/g, respectively, i.p.) and placed on their right sides. Thirty μl of virus solution was slowly delivered to the right nasal cavity by applying multiple 6 μl doses over a 45 min period. Solution was delivered through polyethylene tubing (0.5mm inside diameter) connected to a 10 μl syringe, with the tubing inserted 8-10 mm into the right nasal cavity. Irrigation was repeated over the next 2 days and mice survived for 4-12 days after the first treatment. Survival intervals are given as days after the first irrigation. Control mice received intranasal administration of sterile PBS (n=2, 7 day survival), or Ad-GFP (1×10^{12} pfu/ml, n=5, 4-7 day survival). Mice treated with AdNT3-GFP (4×10^{9} pfu/ml) were euthanized at 5 (n=5), 7 (n=6), 10 (n=4), and 12 days (n=2) post-treatment. Mice treated with AdNT3-3xHA-IRES-GFP (2×10^{10} pfu/ml) survived 5 (n=5), 7 (n=6), or 10 days (n=2) post-infection.

Detection of fusion peptide expression in vivo

Treated mice were euthanized as described and perfused with 4% PFA in PB. Brains with attached nasal cavities were post-fixed for 2 hrs, decalcified with 0.37 M ethylenediaminetetra-acetic acid (EDTA) for 20 hrs, then placed in 25% sucrose in PB for 48 hrs. To obtain sections with intact olfactory nerve connections, tissue was embedded in 10% gelatin, followed by postfixation and cryoprotection in 4% PFA with 30% sucrose overnight, embedding in OCT compound (Tissue-Tek, Sakura), and freezing in isopentane (-50°C). Brains were stored at -80°C for less than 1 month prior to sectioning. Horizontal sections (30μm) were collected in a cryostat, and processed free-floating. Tissue blocked in 5% normal horse serum (NHS) for 1.5 hrs, followed by overnight incubation in primary antibodies diluted in PBS or Tris-buffered saline containing 5% NHS and 0.3% Triton X-100. The following primary antibodies were used: goat anti-OMP (1:7000, #544-10001, Wako Chemicals, Richmond, VA), goat anti-doublecortin (DCX, 1:500, #sc-8066, Santa Cruz Biotech), mouse anti-HA (0.5 μg/ml; Covance), rabbit anti-HA (1:200; #C29F4, Cell Signaling Technologies), rabbit anti-HA (1:250; #H6908; Sigma), our rabbit NT3 antibody (1:800) and goat antibody to the extracellular domain of TrkC (1:250, #AF1404, R and D Systems, Minneapolis, MN). Incubation in AlexaFluor594- or 568- and/or 488-conjugated donkey secondary antibodies (1:1000) was carried out for 2 hrs, followed by counterstaining with Vectashield containing DAPI. Additional sections incubated with mouse anti-HA were processed with an AlexaFluor555-conjugated goat anti-mouse $F(ab')_2$ fragment secondary (Invitrogen) to test for non-specific anti-mouse staining by secondary antibodies. Controls also included omission of the primary HA antibodies, substitution of mouse anti-HA with mouse IgG in the primary incubation (1μg/ml; #I-2000, Vector Laboratories), and preabsorbtion of HA antibodies with 30μg/ml HA peptide (#12149, Sigma) overnight at 4°C. Sections were examined and images collected using confocal and fluorescence microscopy. Unless otherwise specified, all confocal images were collected at 4μm optical section thickness (~2 airy units) or less. Four additional mice treated with AdNT3-GFP (n=2) or AdNT3-3xHA (n=2) were perfused with 2% PFA with 0.2% PBQ, and sections were processed for immunoperoxidase staining using our rabbit antibody to NT3 as described. Tissue was examined using bright-field, fluorescence, and/or confocal microscopy. Figures were assembled in Adobe Photoshop CS3, with adjustments made for size, brightness, and contrast.

Ultrastructural localization of NT3-GFP in sensory axons: Pre-embedding immunogold-silver labeling

Two adult female C57Bl6 mice received intranasal treatment with AdNT3-GFP over 3 days as described. A third mouse received intranasal sterile saline infusions. On the sixth day after the first treatment, mice were euthanized as described and perfused with cold PB followed by 4% PFA. Carcasses were stored at 4°C overnight. Brains were dissected and postfixed in 4% PFA for 3 days, then rinsed for 30 min in PBS. Coronal vibratome sections through the olfactory bulbs were cut at 50 μm and processed for pre-embedding immunogold-silver detection of the fusion protein in sensory axons, with modifications of the procedure described in Cheng et al. (1995). Sections were rinsed in PB, followed by 0.1 M glycine, and incubated in 0.1% sodium borohydride for 15 min. To optimize antibody penetration, tissue was then permeabilized in 0.05% Triton X-100 for 40 min. After rinsing in PBS, sections incubated in Aurion goat blocker solution (0.5% BSA, 0.1% cold water fish serum, 0.5% normal goat serum, EM Sciences, Hatfield, PA) for 25 min. Sections rinsed twice in 0.15% acetylated BSA-c (Aurion) in PBS, followed by 20 hr incubation in rabbit anti-GFP at 4°C (1:400; #AB6556, Abcam) diluted in PBS containing 0.15% acetylated BSA-c. Tissue incubated overnight at 4°C in Ultra Small (0.8-1.0 nm) immunogold F(ab')2 fragment of goat anti-rabbit IgG (1:100, Aurion) diluted in PBS with BSA-c. After washing, sections were postfixed in 2.5% gluteraldehyde for 2 hrs, rinsed in water, and treated with silver enhancing solution for 5 min (Ted Pella, Redding, CA). Sections were rinsed, counterstained, fixed with 0.5% OsO_4, and dehydrated through graded alcohols. Embedding was carried out at 65°C according to standard techniques using propylene oxide and Epon-12-based resin. Ultramicrotome sections were cut from trimmed blocks at 60-80 nm, and post-stained with uranyl acetate and lead citrate on grids for TEM imaging. The olfactory nerve layer was examined with a Phillips CM-10 transmission electron microscope and images were collected using a Gatan digital camera. Controls included processing sections from the saline-treated mouse, and sections from adenovirus-treated mice without the GFP antibody.

Intrabulbar administration of AlexaFluor568-conjugated peptide

Retrograde transport of rhodamine-conjugated BDNF to forebrain cholinergic neurons has been demonstrated following its injection into the bulb's granule cell layer (Jezierski and Sohrabji, 2003). To test if bulbar neurons could acquire exogenous NT3, administration of AlexaFluor568 (AF568)-conjugated NT3 was performed in vivo using glomerular injections. Recombinant human NT3 (mature form, Peprotech Inc.) was custom labeled with AF568 by Invitrogen. Conjugated peptide was diluted in sterile 0.1M PB to 50ng/μl. Three female C57Bl6 mice were anesthetized and received stereotaxic injections of 200 nl of peptide into the medial glomerular layer of each bulb (coordinates: 3.9 mm anterior to Bregma, 0.09 mm left and right of midline suture, 2.2 mm below skull surface). Three control mice were injected bilaterally with 200 nl of AF568-conjugated goat anti-rabbit $F(ab')_2$ fragments (Invitrogen, diluted to 50μg/ml; preabsorbed against mouse serum and hybridoma proteins). Mice were euthanized 3 hrs later, perfused with 4% PFA, and the brains dissected, post-fixed and cryoprotected as described. Horizonatal cryosections (30μm) were slide-mounted, coverslipped with Vectashield containing DAPI, and were examined using fluorescence and confocal microscopy.

Results

Olfactory sensory neurons express endogenous NT3 mRNA and protein

To quantify relative levels of OSN neurotrophin expression in normal adult mice, Q-RT-PCR amplification was performed using RNA isolated by laser-capture microdissection. As shown in figure 1B, NT3 transcripts were ~2.3-fold more abundant than those of NGF and

BDNF. Mean Ct values were as follows: beta-actin=21.33, NT3=27.30, BDNF=28.69, NGF=28.66, NT4=39.26, OMP=15.01, no template controls=no Ct. NT4 transcripts were not detected. OMP transcripts were at least 16-fold more abundant than beta-actin, verifying that our samples were enriched for high quality, mature OSN transcripts. This data is consistent with the larger numbers of beta-galactosidase+ OSNs reported in NT3-lacZ reporter mice compared to BDNF-lacZ animals (Vigers et al. 2003; Clevenger et al., 2008). Our results are also consistent with gene expression profiling data showing that NT3 is expressed at higher levels in the mouse OE relative to the other neurotrophins, and that its expression declines following bulbectomy as OSNs degenerate (Shetty et al., 2005; Magklara et al., 2011). As expected, hippocampal samples exhibited much higher neurotrophin transcript levels (except NT4, Fig. 1C). Relative levels were consistent with results of in situ cRNA hybridization studies, with BDNF the most abundant by far (BDNF>NGF>NT3>NT4; Lauterborn et al., 1995; Mudo et al., 1996). Using about half the amount of RNA used for OSN samples, mean Ct values for hippocampus were as follows: beta-actin=17.87, NT3=31.82, BDNF=26.15, NGF=29.45, and NT4=no Ct.

To localize endogenous NT3 protein, we generated a polyclonal antibody against three amino acid sequences within mature NT3 having minimal homology to BDNF and NGF sequences. As shown in figure 1D, Western blot analysis confirmed that this antibody does not cross react with other neurotrophins. Immunoperoxidase staining produced labeling in the somata and dendrites of a subpopulation of OSNs when performed using 2% PFA fixation with PBQ (Figs. 1E-G). This fixation facilitates immunostaining for neurotrophins in rodent brain (Conner et al., 1997). Lighter staining was also seen in axon bundles deep to the epithelium (Fig. 1G), and in the olfactory bulb, faint immunoreactivity (IR) was observed in the neuropil of glomeruli, with variations in staining intensity seen across the population (Fig. 1H). Specific staining was not observed elsewhere in the bulb, and staining in the olfactory nerve was equivalent to non-specific, background levels seen in control sections processed without the primary antibody. Labeling in the OE resembled that reported for Santa Cruz antibody sc-547, and was similarly reduced by fixation with 4% PFA, however unlike this previous report, we did not observe IR in sustentaclular cells (Feron et al., 2008). The pattern of OSN staining we observed was similar to that reported for histochemical detection of beta-galactosidase in adult, heterozygous NT3-lacZ mice (Vigers et al., 2003). Labeling of other neuronal populations known to express NT3, including cerebellar Purkinje cells (Fig. 1I), and more faintly, mossy fibers in the dentate gyrus (Fig. 1J), was detected as well (Das et el., 2001). Preabsorption of the antibody with the mature peptide (hrNT3) eliminated specific labeling, and incubation in pre-immune serum produced non-specific staining in the OE (Fig. 1J-K). As described below, peptide preabsorption also eliminated Western blot detection of recombinant NT3 peptide, as well as mature NT3 contained in lysates from COS7 cells expressing epitope-tagged NT3 (Fig. 2).

NT3 fusion proteins are synthesized, secreted, and exhibit biological activity in vitro

To monitor the trafficking of NT3 in the olfactory pathway, we utilized adenovirus vectors encoding NT3 fusion peptides. Appropriate expression of the constructs in mammalian cells was verified by Western blot analyses of lysates from cultured COS7 cells following infection. As shown in figure 2A, blots probed with the Santa Cruz NT3 antibody confirmed that infected cells expressed fusion proteins of the predicted molecular mass for proNT3-GFP (~59 kDa) and proNT3-3xHA (~37-39 kDa). These larger proforms of the peptides predominated, and the HA-tagged sequence appeared as multiple bands indicative of variable glycosylation, as has been observed for native and epitope-tagged proBDNF (Teng et al., 2005). The mature forms of the tagged factors were less abundant in the lysates. A faint band for mature NT3-GFP was observed at ~43 kDa, and a band for mature NT3-3xHA was seen at ~17kDa when larger amounts of protein were probed. Detection of mature

hrNT3 peptide and of HA-tagged NT3 in COS cell lysates was eliminated by preabsorbtion of our rabbit NT3 antibody with hrNT3, demonstrating its specificity (Fig. 2B).

The intracellular distribution of the expressed fusion proteins was monitored in COS7 and N2a neuroblastoma cells (Fig. 3A-K). COS cells infected with GFP-encoding control virus exhibited typical GFP fluorescence distributed throughout the cell body, including the nucleus (Fig. 3A). Cells infected with AdNT3-GFP displayed distinct fluorescent puncta concentrated in the Golgi apparatus near the nucleus (Fig. 3B). N2a cells showed a similar perinuclear localization of NT3-GFP, and additionally displayed punctate GFP in their neurites, suggesting a vesicular distribution (Fig. 3C). To determine if the fusion protein was contained in secretory vesicles, infected N2a cells were processed for immunodetection of secretogranin II, a protein in dense core secretory vesicles that co-localizes with neurotrophins and participates in peptide packaging (Haubensak et al., 1998; Wu et al., 2004). As shown in figures 3D-F, confocal imaging verified co-localization of GFP and secretogranin II, demonstrating transport of the NT3 fusion protein in secretory vesicles within neurites. N2a cells expressing the biscistronic sequence NT3-3xHA-IRES-GFP exhibited similar punctate labeling in neurites when stained with HA antibody, while GFP fluorescence was seen throughout the cells (Figs. 2G-K). To verify peptide secretion, levels of NT3 in media collected from infected COS cells were assayed by ELISA using a method that detects both pro- and mature NT3. Total NT3 measured 942 +/- 54 pg/ml in undiluted samples from AdNT3-GFP infected cultures, while in samples from Ad-GFP infected cultures, values measured 4.8 +/- 0.8 pg/ml ($p<0.001$, unpaired t-tests).

Proprioceptive DRG neurons express TrkC and exhibit enhanced neurite outgrowth in vitro when stimulated with NT3 (Dijkhuizen et al., 1997). Using dissociated neonatal rat DRG neurons, we confirmed that CM from COS7 cells expressing NT3-3xHA promoted neurite outgrowth, as well as DRG neuron survival. DRG neurons maintained in 10% FCS for 2.5 days appeared healthy, and most adopted a unipolar or bipolar morphology with short processes. Two days after transfer to 1% FCS, cells in untreated control cultures were fewer in number and some showed evidence of fragmentation. Cultures treated with CM from Ad-GFP-infected COS cells were similar. In contrast, cultures treated with NT3 or CM from NT3-3xHA expressing cells contained more intact neurons with processes, although fewer than observed after 2 days in 10% FCS. Morphology typically was bipolar, but neurons with 3-4 neurites were also evident, and many formed contacts with other neurons. Measures of neurite length showed a significant outgrowth enhancement with 2 days of NT3 or NT3-3xHA CM administration, compared to both control culture conditions ($p<0.0001$, one-way ANOVA; $p<0.001$, Bonferroni's post-hoc tests). Mean length of the longest neurite was 62.5 +/-5.6 μm (SEM) in untreated cultures, and 68.0 +/- 7.1 μm in cultures treated with CM from Ad-GFP-infected COS cells ($p>0.05$, Bonferroni's test). DRG neurons treated with NT3 peptide averaged neurite lengths of 132.4 +/-7.5 μm, while those treated with media from NT3-3xHA infected cells averaged 133.6 +/-6.6 μm ($p>0.05$, Bonferroni's test). Cultures were maintained for an additional 2 days to monitor further differentiation, and by this time neurons in control cultures were scarce. Small numbers of surviving neurons with stunted processes were seen (Fig. 3L). In cultures treated with NT3 or NT3-3xHA, surviving neurons remained at 4 days, although fewer were seen at this time than at 2 days. In both the trophic factor-exposed cultures, cells displayed long processes, prominent growth cones, and formed neuritic networks. All exhibited 2-4 neurites, and some displayed branching as well (Fig. 3M). These results demonstrate that NT3-3xHA is functionally capable of stimulating Trk receptor-mediated neurite growth in a subpopulation of DRG neurons.

Adnenovirus-infected olfactory sensory neurons express NT3 fusion proteins in vivo

We hypothesized that in much the same way endogenous BDNF and NT3 act as anterograde trophic signals in the optic nerve pathway, NT3 synthesized by OSNs might be transported

anterogradely for release in the olfactory bulb (von Bartheld and Butowt, 2000; Menna et al., 2003). Immunodetection of NT3 in glomeruli suggests this is the case, but does not rule out the possibility that glomerular NT3-IR originates from other sources, such as centrifugal projections. We adopted the strategy of in vivo gene transfer to detect NT3 distribution in the olfactory pathway using GFP and HA epitope tags. Following intranasal application of the adenoviruses, GFP was detected in OSNs and sustentacular cells by 4 days, with peak expression seen in the right OE at 7-10 days (Fig. 4A). Though viruses were applied to the right nasal cavity, more restricted infection was detected in portions of the left nasal mucosa as well, indicating spillover via the pharynx or the external nares during treatment. Saline irrigation had no detectable effect on the OE.

Comparison of intracellular GFP distribution showed that sensory neurons infected by the control virus displayed diffuse fluorescence throughout, whereas those expressing NT3-GFP showed punctate labeling in the cell body, with dense accumulation of fluorescence in the Golgi apparatus (Figs. 4A-D). As shown in figure 4D, fluorescent puncta were also detected within the dendrite and proximal axon segment. This distribution extended into the more distal axon compartment, and axons containing vesicular-like GFP labeling could be followed as they exited the OE, and converged into bundles beneath the lamina propria (Fig. 4E). As shown in figure 4F, the GFP+ puncta could be localized to OMP+ axons. This axonal distribution of NT3-GFP suggested that the fusion peptide was associated with secretory vesicles, however the secretogranin II antibody did not produce staining due to tissue EDTA treatment. We therefore performed pre-embedding immunogold-silver labeling to localize GFP-IR at the ultrastructural level. Within cross sections through bundles of sensory axons in portions of the olfactory nerve layer, dense clusters of gold-silver deposits were observed in tissue processed with the GFP antibody (Fig. 4G), similar to those seen with immunogold-silver labeling of presynaptic BDNF in DRG afferents in spinal cord and mossy fibers in hippocampus (Luo et al., 2001; Dieni et al., 2012). Deposits were typically large and dense, tending to obscure underlying features, but smaller gold-silver particles could be resolved in presumptive secretory vesicles for those that were less heavily labeled (inset in Fig. 4G). Control sections from the saline-treated mouse did not contain these axonal silver deposits.

Axonal transport of NT3 fusion proteins to the olfactory bulb

At 5 days post-infection and thereafter, GFP was detected in the glomerular layer of AdNT3-GFP treated mice, particularly in lateral portions of the right bulb as seen in horizontal sections, although other bulb areas also showed labeling (Fig. 5A). As with axonal labeling, glomerular NT3-GFP appeared distinctly punctate (Fig. 5B). Colocalization of GFP with DCX-IR axons was not observed, but immunostaining demonstrated that the distribution of glomerular GFP and OMP-IR overlapped within glomeruli (Fig. 5C). As shown in figure 5D, vesicular-like NT3-GFP labeling could be traced along incoming sensory axons that terminated within glomeruli. In contrast, control mice treated with Ad-GFP showed uniform GFP fluorescence in sensory axons projecting to the bulb (Fig. 5E). Within the bulb, accumulated NT3-GFP appeared restricted to the glomerular neuropil.

As illustrated in figure 6, when nasal irrigation employed AdNT3-3xHA-IRES-GFP, infected sensory neurons exhibited a vesicular-like pattern of HA-IR, similar to that seen with NT3-GFP expression (Figs. 6A-C). We used three different antibodies to HA, including the Sigma rabbit antibody used by Yang et al. (2009) to localize endogenous proBDNF-HA in the hippocampus of transgenic mice. With these antibodies, labeling was again concentrated in the Golgi apparatus, and immunoreactive puncta were distributed in dendrites and proximal axons (Fig. 6B). GFP was distributed throughout neuronal somata and processes, and GFP+ axons could be seen projecting to bulb glomeruli (Fig. 6D’). These targeted glomeruli were also immunoreactive for HA, and both the mouse and rabbit

antibodies produced similar labeling patterns (Figs. 6D-F). In HA+ glomeruli, staining was associated with the neuropil, and in contrast to results seen with NT3-GFP, extended beyond the more limited distribution of individual GFP+ axon terminals, and included juxtaglomerular cells (Figs. 6D”-F). The pattern suggested HA accumulation by local glia or neurons and their processes, and possibly presynaptic terminals. Sections processed without the HA primary antibodies (Fig 6G), with mouse IgG as primary (Fig. 6H), or with preabsorbed HA antibodies (Fig. 6I), did not show specific glomerular staining for HA, however the mouse IgG and mouse HA antibody both produced non-specific staining of ensheathing glia and their processes in the outer olfactory bulb nerve layer (Figs. 6H-J). As illustrated in figures 6J-L”, glomeruli with bright GFP fluorescence throughout displayed distinct HA-IR, while those with few GFP+ fibers showed little or no HA-IR.

Although most HA immunostaining was associated with the glomerular layer, HA-IR was also observed in small numbers of tufted and mitral cells near the most intensely immunoreactive glomeruli. As shown in figures 7A-C, portions of the mitral cell layer deep to GFP+/HA+ glomeruli contained HA+ mitral cells, with dendrites extending toward these glomeruli. Staining was not seen in the granule cell layer. The detection of HA-IR in bulb neurons suggested that these cells may have acquired NT3-3xHA from OSNs over-expressing it. We tested the abilty of mitral cells to accumulate exogenous AF568-tagged NT3 when applied to the glomerular layer, and observed that mitral and tufted cells deep to injection sites, as well as some glomerular neurons, contained immunofluorescence within 3 hours of application (Fig. 7D). Glomerular injections of AF568-conjugated anti-rabbit F(ab”)2 fragments did not produce this labeling, with fluorescence appearing to accumulate in putative ensheathing glia, and in aggregates within the glomerular layer (Fig. 7E).

HA localization in bulb neurons suggested the release of the fusion peptide by sensory afferents, and possible acquisition via postsynaptic TrkC receptors, which are expressed at high levels in the olfactory bulb (Deckner et al., 1993). To confirm that neurons immunoreactive for HA indeed expressed TrkC, we colocalized HA with this receptor using an antibody to the extracellular binding domain. Specificity of the antibody was confirmed by Western blot probing of TrkB immunoprecipitated from mouse cortical lysates (Santa Cruz, TrkB antibody sc-8316, data not shown). Immunofluorescence demonstrated that TrkC localized to neurons distributed in all bulb laminae, with mitral cells showing particularly strong labeling (Fig. 7F). Within the EPL, mitral and tufted cell dendrites were immunoreactive. Dense labeling was observed in the glomerular neuropil (Fig. 7G) and most of this staining appeared to be dendritic (Fig. 7G), with labeled dendrites extending upward from the EPL. A subpopulation of cells bordering glomeruli, putative PG cells based on their size and distribution, were labeled as well (Fig. 7H). In mice with sensory neuron expression of NT3-3xHA, bulb cells immunoreactive for HA were also TrkC+. Double-labeled cells were observed in the glomerular layer, and within the subpopulation of HA+ tufted and mitral cells, with co-labeling seen in somata and dendritic processes (Fig. 7I-I”). Bulbar NT3 immunofluorescence was not observed with 4% PFA fixation of virus-treated mice. In 2 mice expressing NT3-3xHA-IRES-GFP and perfused with 2% PFA/0.2% PBQ, increased NT3-IR was detected in the Golgi apparatus of infected OSNs using immunoperoxidase staining (not shown), while labeling in the nerve layer and bulb was comparable to that seen in control mice. Therefore it is possible that HA-IR reflects non-specific accumulation of liberated HA peptide, rather than secreted NT3-3xHA. The present study did not determine if HA-IR, potentially reflecting proNT3-3xHA, localized to p75+ olfactory ensheathing cells.

Discussion

Localizing neurotrophins in the olfactory pathway has been somewhat complicated by their shared sequence homology, the fact that the peptides can be acquired by cells that do not synthesize them, and variable distributions reported using different antibodies and fixation techniques. NT3-IR has been localized exclusively to sustentacular cells in adult OE with an antibody to the N-terminal region of the peptide (Millipore rabbit anti-NT3; AB1532P; Simpson et al., 2003), or to all but basal OE cells, including most OSNs, with an antibody to a portion of the C-terminal sequence (Santa Cruz rabbit anti-NT3; sc-457; Feron et al., 2008). Characterizing gene expression levels has also been less than straightforward. Heterozygous NT3-lacZ reporter mice show robust beta-galactosidase staining in a subset of mature OSNs, and NT3 mRNA can be detected by standard RT-PCR of mucosa samples, but has not been detected in the OE by in situ cRNA hybridization, or by early OE gene expression profiling studies (Nef et al., 2003; Vigers et al., 2003; Feron et al., 2008; Sametta et al., 2007). However more recent gene expression profiling experiments have reported low levels of NT3 expression in mouse OSNs, and the present laser-capture/Q-PCR results demonstrate this expression as well (Magklara er al., 2011). Taken together with our immunostaining results, similar neuronal NT3-IR reported by Mackay-Sim's group, and the observations made in NT3-lacZ reporter mice, these findings indicate that in adult mice, some OSNs normally express NT3 mRNA, and synthesize NT3 protein (Vigers et al., 2003; Feron et al., 2008). Sensory neurons express a variety of other trophic molecules as well and it has been tempting to speculate that OSN-derived factors provide anterograde support to bulb neurons, in addition to any autocrine/paracrine actions they may exert within the epithelium or olfactory nerve.

That native NT3 can be anterogradely trafficked by the OSNs that express it is supported by localization of the fusion peptides in virus-infected neurons. The tagged factors are packaged in the secretory apparatus, and undergo vesicular axonal transport to the bulb. However within the bulb, the GFP and HA epitopes differed in their distributions. NT3-GFP localized to secretory vesicles both in vitro and in vivo, and we could detect its secretion by infected COS cells, but there was no evidence that the GFP-tagged peptide transferred to bulb neurons. To date, secretion and postsynaptic transfer of a GFP-tagged neurotrophin has been limited to a report of cultured, BDNF-GFP transfected cortical neurons; it has not been demonstrated in vivo (Kohara et al., 2001). Once secreted, the relatively large size of GFP may partially disrupt normal neurotrophin actions, but the tendency of GFP to form disulfide-linked oligomers in secretory vesicles is an additional factor to consider (Molinete et al., 2000; Jain et al., 2001). If such oligomers are secreted, they may limit the ability of the tagged neurotrophin to form homodimers or effectively bind native Trk receptors. Impaired function has been noted for other GFP-tagged proteins (Fucile et al., 2002).

The smaller HA epitope is less likely to interfere with neurotrophin receptor binding, and our DRG culture assays confirmed the Trk-mediated biological activity of the NT3-3xHA. The presence of HA-IR in subsets of bulb neurons is suggestive of NT3-3xHA transfer from sensory axons, similar to the transneuronal transfer seen when exogenous, radio-labeled neurotrophins are released from retinal ganglion cell (RGC) axons to target neurons in the visual pathway (von Bartheld et al., 1996; Butowt and von Bartheld, 2001). As we here, and others shave shown, bulb neurons express both full-length and truncated TrkC, making them capable of NT3 binding, and their acquisition of AF568-tagged NT3 applied to the glomerular layer supports this (Deckner et al., 1993; Menn et al., 1998). They do not express the p75 receptor, which has greater affinity for the proforms of the neurotrophins, and is expressed by olfactory ensheathing glia (Gong et al., 1994; Bianco et al., 2004; Teng et al., 2005; Galvao et al., 2008). Combined localization of TrkC, HA, and NT3 in our material was not possible with the fixation used, so it remains possible that the HA epitope was

cleaved from NT3, or liberated by protein degradation, and accumulated in bulb neurons non-specifically. We consider this unlikely given the widespread experimental use of HA to tag proteins in a variety of systems. Unlike FLAG peptide, another widely-used epitope tag that can be cleaved by enterokinase, there is no report of enzymatic cleavage of HA, and the persistence of intact proBDNF-HA has been demonstrated in mouse brain in vivo (Einhauer and Jungbauer, 2001; Yang et al., 2009). Nevertheless, electron microscopic analyses will be needed to determine if HA or NT3 specifically localize to Trk-containing endosomal structures within bulb neuron dendrites in virus-treated mice, in order to definitively demonstrate postsynaptic transfer (Valdez et al., 2005).

That innervating olfactory axons exert an anterograde tropic influence on the olfactory bulb is well established. Sensory neuron innervation is critical to the morphological and neurochemical development of the bulb, as well as its maintenance in later life (Brunjes and Frazier 1986; De Carlos et al., 1995; Gong and Shipley, 1995). Bulb formation is severely disrupted if sensory afferents fail to contact the telencephalon (Jimenez et al., 2000). Postnatally, prolonged denervation leads to reduced numbers of mitral/tufted and PG cells, dendritic atrophy, and decreased expression of phenotypic markers, including tyrosine hydroxylase (Baker et al., 1983; Couper Leo et al., 2000, Couper Leo and Brunjes, 2003). Some of these outcomes are also seen with sensory deprivation by naris occlusion (Brunjes, 1994; Fiske and Brunjes, 2001; Matsutani and Yamamoto, 2000), demonstrating that anterograde effects include activity-dependent mechanisms that can be reinstated when deprivation is reversed, even in adulthood (Henegar and Maruniak, 1991; Cummings et al., 1997; Bastien-Dionne et al., 2010; Cummings and Belluscio, 2010). Afferent release of neurotrophins is activity-dependent, particularly in response to patterned, high-frequency stimulation, and if this holds true for NT3 or other factors made by OSNs, such a mechanism could contribute to the development or maintenance of innervated bulb neurons (Lever et al., 2001; Wang et al., 2002; Langenhan et al., 2005; Matsuda et al., 2009; Jia et al., 2010).

In the rodent visual pathway, NT3 and BDNF expressed by RGCs act in an autocrine fashion to promote maturation of retinotectal synapses, as well as the growth of RGC axons during refinement of their geniculate projections (Menna et al., 2003; Wang et al., 2003). Optic nerve-derived BDNF also acts as an anterograde survival factor for tectal neurons; normal levels of apoptosis in developing tectum are reduced when afferent BDNF is increased, while blocking BDNF signaling at retinal inputs exacerbates tectal cell death (Caleo et al., 2000; Spalding et al., 2002). In the olfactory pathway, the specific actions of neurotrophins are not well characterized. NT3 is not required for embryonic development of the bulb or epithelium, which appear grossly normal in neonatal NT3 null mice, however these animals exhibit an increased incidence of apoptotic, mature OSNs (Nef et al., 2001; Simpson et al., 2003). Cultured embryonic mitral/tufted cells do not show morphological responses to NT3, but when administered to cultured OSNs, NT3 stimulates Erk1/2 and Akt kinase phosphorylation, and promotes their survival (Holcomb et al., 1995; Simpson et al., 2003; Tran et al., 2008). Effects of NT3 gene inactivation have not been studied in older mice due to early lethality, but mature OSNs in adult animals express TrkC, suggesting that survival effects may also operate at later ages to help maintain the population through autocrine mechanisms (Feron et al., 2008). Additionally, NT3 has reported trophic effects on olfactory ensheathing glia (Bianco et al., 2004).

Neurotrophins are well known as survival/maturation factors for neurons in the developing peripheral nervous system, and for populations of neurons in developing brain as well, including the aforementioned tectal neurons (McAllister et al., 1996, 1999; Huang and Reichardt, 2001; Horch and Katz 2002). Recent evidence provides support for the notion that neurotrophins also help regulate the survival and development of new neurons in adult

brain. Such actions have been documented in brain areas that undergo adult neurogenesis, including the rodent hippocampus and song control centers of the avian forebrain, where subpopulations of new cells are selected for long-term survival (Alvarez-Borda et al., 2004; Shimazu et al., 2006; Chan et al., 2008; Wissman and Brenowitz, 2009). NT3 has been specifically implicated in the integration of adult-born neurons in both of these systems (Johnson et al., 1997; Shimazu et al., 2006). The olfactory bulb similarly integrates new neurons throughout life, as new new granule and PG cells are generated from progenitors in the forebrain SVZ (Petreanu and Alvarez-Buylla, 2002; Lledo and Saghatelyan, 2005; Nissant and Pallotto, 2011). About half of new PG cells undergo apoptosis within 5 weeks of their arrival in the glomerular layer, as synapses with OSNs become established (Winner et al., 2002; Whitman and Greer, 2007; Grubb et al., 2008; Mouret et al., 2009). Sensory deprivation increases their loss, while odor stimulation/experience promotes their survival, and accelerates their dendritic development within topographically activated regions (Alonso et al., 2006; Mandairon et al., 2006; Linveh et al., 2009; Sawada et al., 2011). Like the developing tectum, trophic signals from innervating sensory axons, including NT3, may regulate the survival and maturation of these developing, adult-born neurons as they functionally integrate within glomerular networks, particularly if such factors are secreted in an activity-dependent manner. Additional experiments will be needed to test whether changes in NT3 availability in the adult olfactory pathway impact the survival, phenotype or morphological maintenance and plasticity of bulb neurons contacted by olfactory sensory axons.

Conclusions

Our findings provide evidence that OSNs synthesize and can anterogradely transport NT3 to the adult olfactory bulb. OSNs express endogenous NT3, and express and sort NT3 fusion proteins to the secretory pathway following adenovirus-mediated gene transfer in vivo. Localization of the fusion proteins demonstrates their anterograde axonal transport to terminals in olfactory bulb glomeruli. Our finding that the HA epitope can be detected in a subset of bulb neurons raises the possibility that OSN-supplied NT3-3xHA can be released to and acquired by postsynaptic neurons in vivo. Our findings are similar to those described in the developing visual system, where optic nerve-derived neurotrophins function as anterograde trophic signals for central target neurons (von Bartheld et al., 1996; von Bartheld and Butowt, 2000; Caleo et al., 2000). The mechanisms controlling OSN release of NT3, and its postsynaptic effects, remain to be experimentally determined, but given the known roles of neurotrophins in other neural systems, this factor may be one of the many molecular signals that contribute to the lifelong plasticity of the primary olfactory pathway.

Acknowledgments

Supported by National Institute of General Medical Sciences grant GM073621, and National Institute of Deafness and Communication Disorders grant DC010485 to KMG. Special thanks to Dr. Charles Ribak, Dr. Vijaya Iragavarapu-Charyulu, Paul Adedoyin and Zhiyin Shan for their expertise and technical assistance, and to the C.E.S. Schmidt Foundation for their support of the FAU College of Medicine RT-PCR and laser confocal imaging instrumentation.

References

Adachi N, Kohara K, Tsumoto T. Difference in trafficking of brain-derived neurotrophic factor between axons and dendrites of cortical neurons, revealed by live-cell imaging. BMC Neurosci. 2005; 6:42. [PubMed: 15969745]

Alonso M, Viollet C, Gabellec MM, Meas-Yedid V, Olivo-Marin JC, Lledo PM. Olfactory discrimination learning increases the survival of adult-born neurons in the olfactory bulb. J Neurosci. 2006; 26:10508–13. [PubMed: 17035535]

Alvarez-Borda B, Haripal B, Nottebohm F. Timing of brain-derived neurotrophic factor exposure affects life expectancy of new neurons. Proc Natl Acad Sci U S A. 2004; 101:3957–61. [PubMed: 15004273]

Ardiles Y, de la Puente R, Toledo R, Isgor C, Guthrie K. Response of olfactory axons to loss of synaptic targets in the adult mouse. Exp Neurol. 2007; 207:275–88. [PubMed: 17674970]

Baj G, Leone E, Chao MV, Tongiorgi E. Spatial segregation of BDNF transcripts enables BDNF to differentially shape dendritic compartments. Proc. Natl. Acad. Sci. USA. 2011; 108:16813–8. [PubMed: 21933955]

Baker H, Kawano T, Margolis FL, Joh TH. Transneuronal regulation of tyrosine hydroxylase expression in olfactory bulb of mouse and rat. J Neurosci. 1983; 3:69–78. [PubMed: 6130133]

Baquet ZC, Gorski JA, Jones KR. Early striatal dendrite deficits followed by neuron loss with advanced age in the absence of anterograde cortical brain-derived neurotrophic factor. J Neurosci. 2004; 24:4250–8. [PubMed: 15115821]

Bastien-Dionne PO, David LS, Parent A, Saghatelyan A. Role of sensory activity on chemospecific populations of interneurons in the adult olfactory bulb. J Comp Neurol. 2010; 518:1847–61. [PubMed: 20235091]

Bianco JI, Perry C, Harkin DG, Mackay-Sim A, Feron F. Neurotrophin-3 promotes purification and proliferation of human olfactory ensheathing cells from human nose. Glia. 2004; 45:111–123. [PubMed: 14730705]

Brigadski T, Hartmann M, Lessmann V. Differential vesicular targeting and time course of synaptic secretion of the mammalian neurotrophins. J. Neurosci. 2005; 25:7601–14. [PubMed: 16107647]

Brunjes PC, Frazier LL. Maturation and plasticity in the olfactory system of vertebrates. Brain Res. 1986; 396:1–45. [PubMed: 3518870]

Brunjes PC. Unilateral naris closure and olfactory system development. Brain Res Rev. 1994; 19:146–60. [PubMed: 8167658]

Butowt R, von Bartheld CS. Sorting of internalized neurotrophins into an endocytic transcytosis pathway via the Golgi system: Ultrastructural analysis in retinal ganglion cells. J. Neurosci. 2001; 21:8915–30. [PubMed: 11698603]

Caleo M, Menna E, Chierzi S, Cenni MC, Maffei L. Brain-derived neurotrophic factor is an anterograde survival factor in the rat visual system. Curr Biol. 2000; 10:1155–61. [PubMed: 11050383]

Carter LA, Roskams AJ. Neurotrophins and their receptors in the primary olfactory neuraxis. Microsc Res Tech. 2002; 58:189–96. [PubMed: 12203697]

Chan JP, Cordeira J, Calderon GA, Iyer LK, Rios M. Depletion of central BDNF in mice impedes terminal differentiation of new granule neurons in the adult hippocampus. Mol Cell Neurosci. 2008; 39:372–83. [PubMed: 18718867]

Cheng PY, Svingos AL, Wang H, Clarke CL, Jenab S, Beczkowska IW, Inturrisi CE, Pickel VM. Ultrastructural immunolabeling shows prominent presynaptic vesicular localization of delta-opioid receptor within both enkephalin- and nonenkephalin-containing axon terminals in the superficial layers of the rat cervical spinal cord. J Neurosci. 1995; 15:5976–88. [PubMed: 7666182]

Clevenger AC, Salcedo E, Jones KR, Restrepo D. BDNF promoter-mediated beta-galactosidase expression in the olfactory epithelium and bulb. Chem Senses. 2008; 33:531–9. [PubMed: 18495654]

Conner JM, Lauterborn JC, Yan Q, Gall CM, Varon S. Distribution of brain-derived neurotrophic factor (BDNF) protein and mRNA in the normal adult rat CNS: evidence for anterograde axonal transport. J Neurosci. 1997; 17:2295–313. [PubMed: 9065491]

Conner JM, Franks KM, Titterness AK, Russell K, Merrill DA, Christie BR, Sejnowski TJ, Tuszynski MH. NGF is essential for hippocampal plasticity and learning. J Neurosci. 2009; 29:10883–9. [PubMed: 19726646]

Couper Leo JM, Devine AH, Brunjes PC. Focal denervation alters cellular phenotypes and survival in the developing rat olfactory bulb. J Comp Neurol. 2000; 417:325–36. [PubMed: 10683607]

Couper Leo JM, Brunjes PC. Neonatal focal denervation of the rat olfactory bulb alters cell structure and survival: a Golgi, Nissl and confocal study. Dev Brain Res. 2003; 140:277–86. [PubMed: 12586433]

Cowan CM, Thai J, Krajewski S, Reed JC, Nicholson DW, Kaufmann SH, Roskams AJ. Caspases 3 and 9 send a pro-apoptotic signal from synapse to cell body in olfactory receptor neurons. J. Neurosci. 2001; 21:7099–109. [PubMed: 11549720]

Cummings DM, Henning HE, Brunjes PC. Olfactory bulb recovery after early sensory deprivation. J Neurosci. 1997; 17:7433–40. [PubMed: 9295389]

Cummings DM, Belluscio L. Continuous neural plasticity in the olfactory intrabulbar circuitry. J Neurosci. 2010; 30:9172–8. [PubMed: 20610751]

Das KP, Chao SL, White DL, Haines WT, Harry GJ, Tilson HA, Barone S. Differential patterns of nerve growth factor, brain-derived neurotrophic factor and neurotrophin-3 mRNA and protein levels in developing regions of rat brain. Neuroscience. 103:739–761. [PubMed: 11274792]

De Carlos JA, López-Mascaraque L, Valverde F. The telencephalic vesicles are innervated by olfactory placode-derived cells: a possible mechanism to induce neocortical development. Neuroscience. 1995; 68:1167–78. [PubMed: 8544990]

Dean C, Huisheng L, Dunning FM, Chang PY, Jackson MB, Chapman ER. Synaptotagmin-IV modulates synaptic function and long-term potentiation by regulating BDNF release. Nature Neuroscience. 2009; 12:767–76.

Deckner ML, Frisén J, Verge VM, Hökfelt T, Risling M. Localization of neurotrophin receptors in olfactory epithelium and bulb. Neuroreport. 1993; 5:301–4. [PubMed: 8298092]

Deckner ML, Risling M, Frisén J. Apoptotic death of olfactory sensory neurons in the adult rat. Exp. Neurol. 1997; 143:132–40. [PubMed: 9000452]

Dieni S, Matsumoto T, Dekkers M, Rauskolb S, Ionescu MS, Deogracias R, Gundelfinger ED, Kojima M, Nestel S, Frotscher M, Barde YA. BDNF and its pro-peptide are stored in presynaptic dense core vesicles in brain neurons. J Cell Biol. 2012; 196:775–88. [PubMed: 22412021]

Dijkhuizen PA, Hermens WTJMC, Teunis MAT, Verhaagen J. Adenoviral vector-directed expression of neurotrophin-3 in rat dorsal root ganglion explants results in a robust neurite outgrowth response. J. Neurobiol. 1997; 33:172–84. [PubMed: 9240373]

Egan MF, Kojima M, Callicott JH, Goldberg TE, Kolachana BS, Bertolino A, Zaitssey E, Gold B, Goldman D, Dean M, Lu B, Weinberger DR. The BDNF val66met polymorphism affects activity-dependent secretion of BDNF and human memory and hippocampal function. Cell. 2003; 112:257–69. [PubMed: 12553913]

Einhauer A, Jungbauer A. The FLAG peptide, a versatile fusion tag for the purification of recombinant proteins. J Biochem Biophys Methods. 2001; 49:455–65. [PubMed: 11694294]

Erickson HS, Albert PS, Gillespie JW, Rodriguez-Canales J, Marston Linehan W, Pinto PA, Chuaqui RF, Emmert-Buck MR. Quantitative RT-PCR gene expression analysis of laser microdissected tissue samples. Nat Protoc. 2009; 4:902–22. [PubMed: 19478806]

Fariñas I, Jones KR, Backus C, Wang XY, Reichardt LF. Severe sensory and sympathetic deficits in mice lacking neurotrophin-3. Nature. 1994; 369:658–61. [PubMed: 8208292]

Feron F, Bianco J, Ferguson I, Mackay-Sim A. Neurotrophin expression in the adult olfactory epithelium. Brain Res. 2008; 1196:13–21. [PubMed: 18234155]

Ferrari CC, Johnson BA, Leon M, Pixley SK. Spatiotemporal distribution of the insulin-like growth factor receptor in the rat olfactory bulb. Neurochem Res. 2003; 28:29–43. [PubMed: 12587661]

Fiske BK, Brunjes PC. Cell death in the developing and sensory-deprived rat olfactory bulb. J Comp Neurol. 2001; 431:311–9. [PubMed: 11170007]

Fleige S, Walf V, Huch S, Prgomet C, Sehm J, Pfaffl MW. Comparison of relative mRNA quantification models and the impact of RNA integrity in quantitative real-time RT-PCR. Biotechnol Lett. 2006; 28:1601–13. [PubMed: 16900335]

Fucile S, Palma E, Martinez-Torres A, Miledi R, Eusebi F. The single-channel properties of human acetylcholine alpha 7 receptors are altered by fusing alpha 7 to the green fluorescent protein. Proc Natl Acad Sci U S A. 2002; 99:3956–61. [PubMed: 11891309]

Galvão RP, Garcia-Verdugo JM, Alvarez-Buylla A. Brain-derived neurotrophic factor signaling does not stimulate subventricular zone neurogenesis in adult mice and rats. J Neurosci. 2008; 28:13368–83. [PubMed: 19074010]

Gong Q, Bailey MS, Pixley SK, Ennis M, Liu W, Shipley MT. Localization and regulation of low affinity nerve growth factor receptor expression in the rat olfactory system during development and regeneration. J Comp Neurol. 1994; 344:336–48. [PubMed: 8063958]

Gong Q, Shipley MT. Evidence that pioneer olfactory axons regulate telencephalon cell cycle kinetics to induce the formation of the olfactory bulb. Neuron. 1995; 14:91–101. [PubMed: 7826645]

Gorski JA, Zeiler SR, Tamowski S, Jones KR. Brain-derived neurotrophic factor is required for the maintenance of cortical dendrites. J Neurosci. 2003; 23:6856–65. [PubMed: 12890780]

Grubb MS, Nissant A, Murray K, Lledo PM. Functional maturation of the first synapse in olfaction: development and adult neurogenesis. J Neurosci. 2008; 28:2919–32. [PubMed: 18337423]

Guthrie KM, Gall CM. Differential expression of mRNAs for the NGF family of neurotrophic factors in the adult rat central olfactory system. J Comp Neurol. 1991; 313:93–102.

Hartmann M, Heumann R, Lessmann V. Synaptic secretion of BDNF after high-frequency stimulation of glutamatergic synapses. EMBO J. 2001; 20:5887–97. [PubMed: 11689429]

Haubensak W, Narz F, Heumann R, Lessmann V. BDNF-GFP containing secretory granules are localized in the vicinity of synaptic junctions of cultured cortical neurons. J Cell Sci. 1998; 111:1483–93. [PubMed: 9580557]

Hayward MD, Bocchiaro CM, Morgan JI. Expression of Bcl-2 extends the survival of olfactory receptor neurons in the absence of an olfactory bulb. Mol Brain Res. 2004; 132:221–234. [PubMed: 15582160]

Henegar JR, Maruniak JA. Quantification of the effects of long-term unilateral naris closure on the olfactory bulbs of adult mice. Brain Res. 1991; 568:230–4. [PubMed: 1814570]

Holcomb JD, Mumm JS, Calof AL. Apoptosis in the neuronal lineage of the mouse olfactory epithelium: regulation in vivo and in vitro. Dev Biol. 1995; 172:307–23. [PubMed: 7589810]

Horch HW, Katz LC. BDNF release from single cells elicits local dendritic growth in nearby neurons. Nat Neurosci. 2002; 5:1177–84. [PubMed: 12368805]

Huang EJ, Reichardt LF. Neurotrophins: roles in neuronal development and function. Annu Rev Neurosci. 2001; 24:677–736. [PubMed: 11520916]

Imayoshi I, Sakamoto M, Ohtsuka T, Kageyama R. Continuous neurogenesis in the adult brain. Dev Growth Differ. 2009; 51:379–86. [PubMed: 19298551]

Jain RK, Joyce PB, Molinete M, Halban PA, Gorr SU. Oligomerization of green fluorescent protein in the secretory pathway of endocrine cells. Biochem J. 2001; 360:645–9. [PubMed: 11736655]

Jezierski MK, Sohrabji F. Estrogen enhances retrograde transport of brain-derived neurotrophic factor in the rodent forebrain. Endocrinology. 2003; 144:5022–9. [PubMed: 12960034]

Jia Y, Gall CM, Lynch G. Presynaptic BDNF promotes postsynaptic long-term potentiation in the dorsal striatum. J Neurosci. 2010; 30:14440–5. [PubMed: 20980601]

Jiménez D, García C, de Castro F, Chédotal A, Sotelo C, de Carlos JA, Valverde F, López-Mascaraque L. Evidence for intrinsic development of olfactory structures in Pax-6 mutant mice. J Comp Neurol. 2000; 428:511–26. [PubMed: 11074448]

Johnson F, Hohmann SE, DiStefano PS, Bottjer SW. Neurotrophins suppress apoptosis induced by deafferentation of an avian motor-cortical region. J Neurosci. 1997; 17:2101–11. [PubMed: 9045737]

Kerman IA, Buck BJ, Evans SJ, Akil H, Watson SJ. Combining laser capture microdissection with quantitative real-time PCR: effects of tissue manipulation on RNA quality and gene expression. J Neurosci Methods. 2006; 153:71–85. [PubMed: 16337273]

Kohara K, Kitamura A, Morishima M, Tsumoto T. Activity-dependent transfer of brain-derived neurotrophic factor to postsynaptic neurons. Science. 2001; 291:2419–23. [PubMed: 11264540]

Kondo K, Suzukawa K, Sakamoto T, Watanabe K, Kanaya K, Ushio M, Yamaguchi T, Nibu K, Kaga K, Yamasoba T. Age-related changes in cell dynamics of the postnatal mouse olfactory neuroepithelium: cell proliferation, neuronal differentiation, and cell death. J Comp Neurol. 2010; 518:1962–75. [PubMed: 20394053]

Kosaka K, Kosaka T. Synaptic organization of the glomerulus in the main olfactory bulb: compartments of the glomerulus and heterogeneity of the periglomerular cells. Anat Sci Int. 2005:80–90. [PubMed: 15960313]

Kuczewski N, Porcher C, Ferrand N, Fiorentino H, Pelligrino C, Kolarow R, Lessmann V, Medina I, Gaiarsa JL. Backpropagating action potentials trigger dendritic release of BDNF during spontaneous network activity. J. Neurosci. 2008; 28:7013–23. [PubMed: 18596175]

Langenhan T, Sendtner M, Holtmann B, Carroll P, Asan E. Ciliary neurotrophic factor-immunoreactivity in olfactory sensory neurons. Neuroscience. 2005; 134:1179–94. [PubMed: 16039789]

Lauterborn J, Berschauer R, Gall C. Cell-specific modulation of basal and seizure-induced neurotrophin expression by adrenalectomy. Neuroscience. 1995; 68:363–78. [PubMed: 7477946]

Leo JM, Devine AH, Brunjes PC. Focal denervation alters cellular phenotypes and survival in the developing rat olfactory bulb. J Comp Neurol. 2000; 417:325–36. [PubMed: 10683607]

Lever IJ, Bradbury EJ, Cunningham JR, Adelson DW, Jones MG, McMahon SB, Marvizón JC, Malcangio M. Brain-derived neurotrophic factor is released in the dorsal horn by distinctive patterns of afferent fiber stimulation. J Neurosci. 2001; 21:4469–77. [PubMed: 11404434]

Linveh Y, Feinstein N, Klein M, Mizrahi A. Sensory input enhances synaptogenesis of adult-born neurons. J Neurosci. 2009; 29:86–97. [PubMed: 19129387]

Lledo PM, Saghatelyan A. Integrating new neurons into the adult olfactory bulb: joining the network, life-death decisions, and the effects of sensory experience. Trends Neurosci. 2005; 28:248–54. [PubMed: 15866199]

Lu B. Acute and long-term synaptic modulation by neurotrophins. Prog Brain Res. 2004; 146:137–50. [PubMed: 14699962]

Luo XG, Rush RA, Zhou XF. Ultrastructural localization of brain-derived neurotrophic factor in rat primary sensory neurons. Neurosci Res. 2001; 39:377–84. [PubMed: 11274736]

Mackay-Sim A, Chuah MI. Neurotrophic factors in the primary olfactory pathway. Prog Neurobiol. 2000; 62:527–59. [PubMed: 10869782]

Magklara A, Yen A, Colquitt BM, Clowney EJ, Allen W, Markenscoff-Papadimitriou E, Evans ZA, Kheradpour P, Mountoufaris G, Carey C, Barnea G, Kellis M, Lomvardas S. An epigenetic signature for monoallelic olfactory receptor expression. Cell. 2011; 145:555–70. (supplemental file). [PubMed: 21529909]

Magrassi L, Graziadei PP. Cell death in the olfactory epithelium. Anat Embryol (Berl). 1995; 192:77–87. [PubMed: 7486003]

Mahalik TJ. Apparent apoptotic cell death in the olfactory epithelium of adult rodents: death occurs at different developmental stages. J Comp Neurol. 1996; 372:457–64. [PubMed: 8873871]

Mandairon N, Sacquet J, Jourdan F, Didier A. Long-term fate and distribution of newborn cells in the adult mouse olfactory bulb: Influences of olfactory deprivation. Neuroscience. 2006; 141:443–51. [PubMed: 16713121]

Matsuda N, Lu H, Fukata Y, Noritake J, Gao H, Mukherjee S, Nemoto T, Fukata M, Poo MM. Differential activity-dependent secretion of brain-derived neurotrophic factor from axon and dendrite. J Neurosci. 2009; 29:14185–98. [PubMed: 19906967]

Matsutani S, Yamamoto N. Differentiation of mitral cell dendrites in the developing main olfactory bulbs of normal and naris-occluded rats. J Comp Neurol. 2000; 418:402–10. [PubMed: 10713569]

McAllister AK, Katz LC, Lo DC. Neurotrophin regulation of cortical dendritic growth requires activity. Neuron. 1996; 17:1057–64. [PubMed: 8982155]

McAllister AK, Katz LC, Lo DC. Neurotrophins and synaptic plasticity. Ann. Rev Neurosci. 1999; 22:295–318. [PubMed: 10202541]

Menn B, Timsit S, Calothy G, Lamballe F. Differential expression of TrkC catalytic and noncatalytic isoforms suggests that they act independently or in association. J Comp Neurol. 1998; 401:47–64. [PubMed: 9802700]

Menna E, Cenni MC, Naska S, Maffei L. The anterogradely transported BDNF promotes retinal axon remodeling during eye specific segregation within the LGN. Mol Cell Neurosci. 2003; 24:972–83. [PubMed: 14697662]

Molinete M, Lilla V, Jain R, Joyce PB, Gorr SU, Ravazzola M, Halban PA. Trafficking of non-regulated secretory proteins in insulin secreting (INS-1) cells. Diabetologia. 2000; 43:1157–64. [PubMed: 11043862]

Mouret A, Lepousez G, Gras J, Gabellec MM, Lledo PM. Turnover of newborn olfactory bulb neurons optimizes olfaction. J Neurosci. 2009; 29:12302–14. [PubMed: 19793989]

Mudò G, Jiang XH, Timmusk T, Bindoni M, Belluardo N. Change in neurotrophins and their receptor mRNAs in the rat forebrain after status epilepticus induced by pilocarpine. Epilepsia. 1996; 37:198–207. [PubMed: 8635431]

Nacher J, Crespo C, McEwen BS. Doublecortin expression in the adult rat telencephalon. Eur J Neurosci. 2001; 14:629–44. [PubMed: 11556888]

Nef S, Lush ME, Shipman TE, Parada LF. Neurotrophins are not required for normal embryonic development of olfactory neurons. Dev Biol. 2001; 234:80–92. [PubMed: 11356021]

Ng BK, Chen L, Mandemakers W, Cosgaya JM, Chan JR. Anterograde transport and secretion of brain-derived neurotrophic factor along sensory axons promote Schwann cell myelination. J. Neurosci. 2007; 27:7597–7603. [PubMed: 17626221]

Nissant A, Pallotto M. Integration and maturation of newborn neurons in the adult olfactory bulb--from synapses to function. Eur J Neurosci. 2011; 33:1069–77. [PubMed: 21395850]

Petreanu L, Alvarez-Buylla A. Maturation and death of adult-born olfactory bulb granule neurons: role of olfaction. J Neurosci. 2002; 22:6106–13. [PubMed: 12122071]

Rauskolb S, Zagrebelsky M, Dreznjak A, Deogracias R, Matsumoto T, Wiese S, Erne B, Sendtner M, Schaeren-Wiemers N, Korte M, Barde YA. Global deprivation of brain-derived neurotrophic factor in the CNS reveals an area-specific requirement for dendritic growth. J Neurosci. 2010; 30:1739–49. [PubMed: 20130183]

Sammeta N, Yu TT, Bose SC, McClintock TS. Mouse olfactory sensory neurons express 10,000 genes. J Comp Neurol. 2007; 502:1138–56. [PubMed: 17444493]

Sawada M, Kaneko N, Inada H, Wake H, Kato Y, Yanagawa Y, Kobayashi K, Nemoto T, Nabekura J, Sawamoto K. Sensory input regulates spatial and subtype-specific patterns of neuronal turnover in the adult olfactory bulb. J Neurosci. 2011; 31:11587–96. [PubMed: 21832189]

Schwob JE, Szumowski KE, Stasky AA. Olfactory sensory neurons are trophically dependent on the olfactory bulb for their prolonged survival. J Neurosci. 1992; 12:3896–919. [PubMed: 1403089]

Schwob JE. Neural regeneration and the peripheral olfactory system. Anat. Rec. 2002; 269:33–49. [PubMed: 11891623]

Shetty RS, Bose SC, Nickell MD, McIntyre JC, Hardin DH, Harris AM, McClintock TS. Transcriptional changes during neuronal death and replacement in the olfactory epithelium. Mol Cell Neurosci. 2005; 30:583–600. [PubMed: 16456926]

Shimazu K, Zhao M, Sakata K, Akbarian S, Bates B, Jaenisch R, Lu B. NT-3 facilitates hippocampal plasticity and learning and memory by regulating neurogenesis. Learn Mem. 2006; 13:307–15. [PubMed: 16705139]

Simpson PJ, Wang E, Moon C, Matarazzo V, Cohen DR, Liebl DJ, Ronnett GV. Neurotrophin-3 signaling maintains maturational homeostasis between neuronal populations in the olfactory epithelium. Mol Cell Neurosci. 2003; 24:858–74. [PubMed: 14697654]

Spalding KL, Tan MM, Hendry IA, Harvey AR. Anterograde transport and trophic actions of BDNF and NT4/5 in the developing rat visual system. Mol Cell Neurosci. 2002; 19:485–500. [PubMed: 11988017]

Teng HK, Teng KK, Lee R, Wright S, Tevar S, Almeida RD, Kermani P, Torkin R, Chen ZY, Lee FS, Kraemer RT, Nykjaer A, Hempstead BL. ProBDNF induces neuronal apoptosis via activation of a receptor complex of p75NTR and sortilin. J Neurosci. 2005; 25:5455–63. [PubMed: 15930396]

Tran H, Chen H, Walz A, Posthumus JC, Gong Q. Influence of olfactory epithelium on mitral/tufted cell dendritic outgrowth. PLoS One. 2008; 3(11):e3816. [PubMed: 19043569]

Valdez G, Akmentin W, Philippidou P, Kuruvilla R, Ginty DD, Halegoua S. Pincher-mediated macroendocytosis underlies retrograde signaling by neurotrophin receptors. J Neurosci. 2005; 25:5236–47. [PubMed: 15917464]

Venkatraman G, Behrens M, Pyrski M, Margolis FL. Expression of Coxsackie-Adenovirus receptor (CAR) in the developing mouse olfactory system. J Neurocytol. 2005; 34:295–305. [PubMed: 16841169]

Verhaagen J, Oestreicher AB, Gispen WH, Margolis FL. The expression of the growth associated protein B50/GAP43 in the olfactory system of neonatal and adult rats. J Neurosci. 1989; 9:683–91. [PubMed: 2918383]

Vigers AJ, Böttger B, Baquet ZC, Finger TE, Jones KR. Neurotrophin-3 is expressed in a discrete subset of olfactory receptor neurons in the mouse. J Comp Neurol. 2003; 463:221–35. [PubMed: 12815759]

von Bartheld CS, Byers MR, Williams R, Bothwell M. Anterograde transport of neurotrophins and axodendritic transfer in the developing visual system. Nature. 1996; 379:830–3. [PubMed: 8587607]

von Bartheld CS, Butowt R. Expression of neurotrophin-3 (NT-3) and anterograde axonal transport of endogenous NT-3 by retinal ganglion cells in chick embryos. J Neurosci. 2000; 20:736–48. [PubMed: 10632603]

Wang X, Butowt R, Vasko MR, von Bartheld CS. Mechanisms of the release of anterogradely transported neurotrophin-3 from axon terminals. J Neurosci. 2002; 22:931–45. [PubMed: 11826122]

Wang X, Butowt R, von Bartheld CS. Presynaptic neurotrophin-3 increases the number of tectal synapses, vesicle density, and number of docked vesicles in chick embryos. J Comp Neurol. 2003; 458:62–77. [PubMed: 12577323]

Whitman MC, Greer CA. Adult-generated neurons exhibit diverse developmental fates. Dev Neurobiol. 2007; 67:1079–93. [PubMed: 17565001]

Winner B, Cooper-Kuhn CM, Aigner R, Winkler J, Kuhn HG. Long-term survival and cell death of newly generated neurons in the adult rat olfactory bulb. Eur J Neurosci. 2002; 16:1681–9. [PubMed: 12431220]

Wissman AM, Brenowitz EA. The role of neurotrophins in the seasonal-like growth of the avian song control system. J Neurosci. 2009; 29:6461–71. [PubMed: 19458217]

Wu YJ, Krüttgen A, Möller JC, Shine D, Chan JR, Shooter EM, Cosgaya JM. Nerve growth factor, brain-derived neurotrophic factor, and neurotrophin-3 are sorted to dense-core vesicles and released via the regulated pathway in primary rat cortical neurons. Neurosci Res. 2004; 75:825–34.

Yang J, Siao CJ, Nagappan G, Marinic T, Jing D, McGrath K, Chen ZY, Mark W, Tessarollo L, Lee FS, Lu B, Hempstead BL. Neuronal release of proBDNF. Nat Neurosci. 2009; 12:113–5. [PubMed: 19136973]

Zhao H, Otaki JM, Firestein S. Adenovirus-mediated gene transfer in olfactory neurons in vivo. J Neurobiol. 1996; 30:521–30. [PubMed: 8844515]

Highlights

- Endogenous neurotrophin-3 is expressed by olfactory sensory neurons in adult mice
- Epitope-tagged NT3 is expressed by sensory neurons after viral-mediated gene transfer
- NT3 fusion proteins are sorted to the secretory pathway in olfactory sensory neurons
- Tagged NT3 is transported in sensory axons to the adult olfactory bulb in vivo
- The epitope tag is detected in some bulb neurons, suggesting postsynaptic transfer

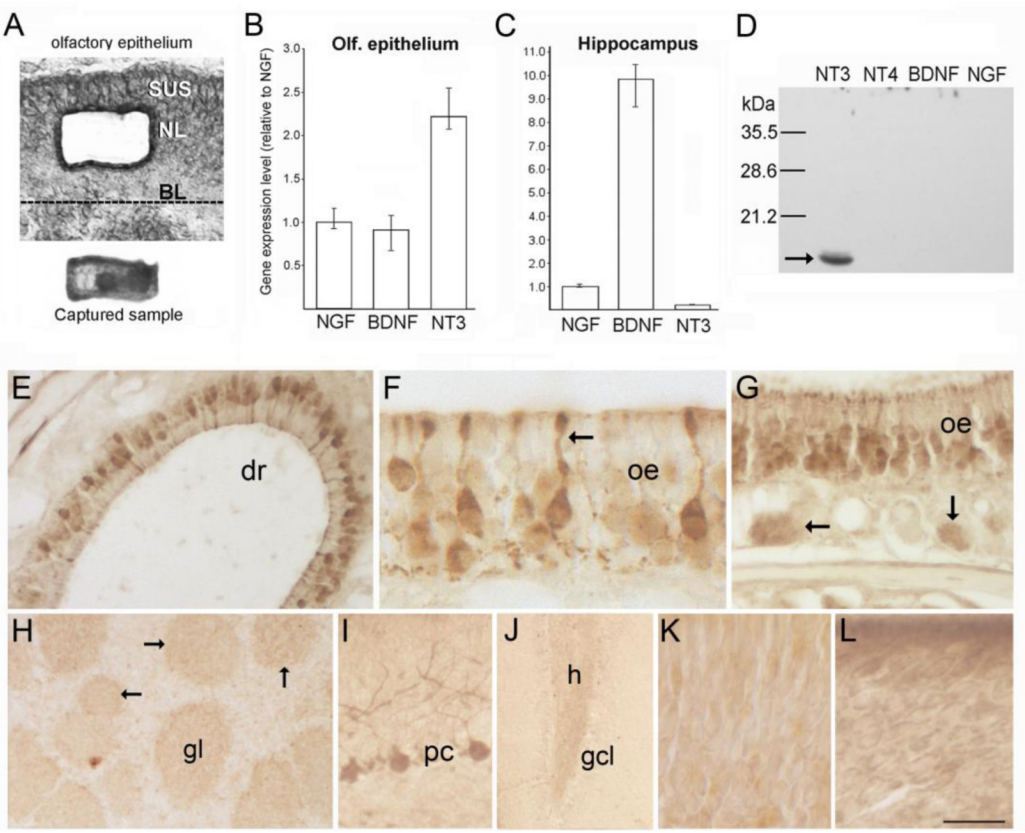

Figure 1.

(A) Photomicrographs of a section through the olfactory epithelium (top) showing the location where cells were isolated by laser microdissection, and the captured cell sample (bottom) as seen on the collection cap. (B-C) Bar graphs showing normalized Q-RT-PCR results obtained from laser-captured OSN samples (B, 45ng total RNA per assay), and dissected hippocampus (C, 20ng total RNA per assay). Mean NGF transcript levels are set to 1.0. Bars indicate mean values calculated for multiple assays, and error bars indicate the range of values obtained across multiple assays for each transcript, rather than statistical error (n=6). (D) Western blot of recombinant neurotrophin peptides (1 μg/lane) demonstrating the specificity of the NT3 antibody. (E-G) Immunostaining for NT3 in the olfactory epithelium (oe). The arrow in F indicates a sensory neuron dendrite, and the arrows in G indicate bundles of more lightly stained sensory axons below the epithelium. (H) In the olfactory bulb, faint staining occurs in the neuropil of glomeruli (gl, and arrows). (I-J) Images showing stained Purkinje cells in cerebellum (I), and more faintly, mossy fibers in the dentate gyrus (J). (K-L) Incubation with pre-absorbed antibody (K) or with pre-immune serum (L) produces non-specific staining in the olfactory epithelium. BL, basal lamina; NL, neuronal layer; SUS, sustentacular cell layer; dr, dorsal recess; gcl, dentate granule cell layer; h, hilus. Bar in K= 40μm in A, 60μm in E, 18μm in F, 41μm in G, 130μm in H, 50μm in I, 100μm in J, and 17 μm in K-L.

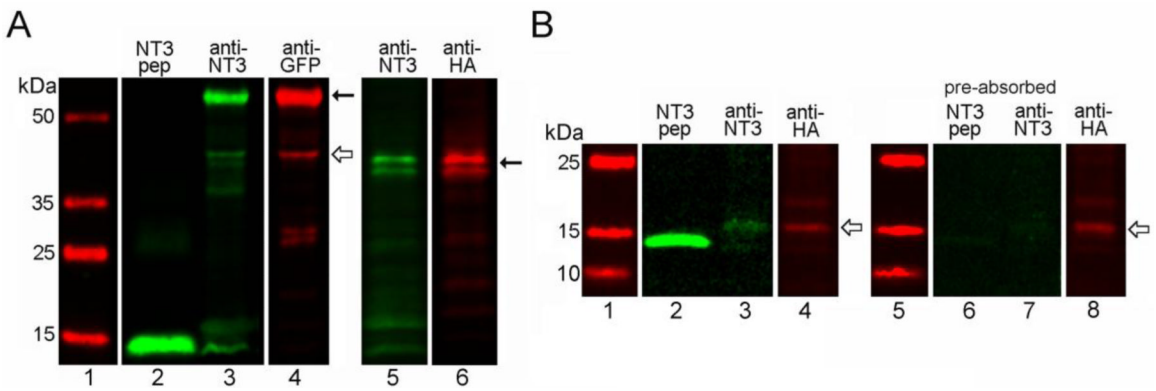

Figure 2.

In vitro expression of NT3 fusion proteins. (A) Western blots of lysates (15μg protein, lanes 3-6) from infected COS7 cells obtained with Santa Cruz NT3 antibody confirming expression of NT3-GFP (left panel, Santa Cruz anti-GFP), and NT3-3xHA (right panel, Covance anti-HA). Lanes 1 and 2 show molecular weight markers and the signal obtained with 100ng of mature, hrNT3 (control peptide), respectively. Solid arrows indicate the proforms of the tagged trophic factor, and the open arrow indicates a smaller band for mature NT3-GFP. Multiple bands seen for proNT3-3xHA reflect variable glycosylation of the protein. (B) Western blots of COS cell lysates (45μg protein, lanes 3-4) obtained with our rabbit NT3 antibody and Covance mouse anti-HA, showing bands for mature NT3-3xHA (open arrows). Lane 1 shows molecular weight markers and lane 2 shows the signal obtained with 30ng of hrNT3 control peptide. Control lanes (6-8) demonstrate that preabsorption of the NT3 antibody with hrNT3 eliminates detection of hrNT3 (30ng, lane 6) and HA-tagged mature NT3 (lane 7), while the HA epitope is still detected (open arrow, lane 8).

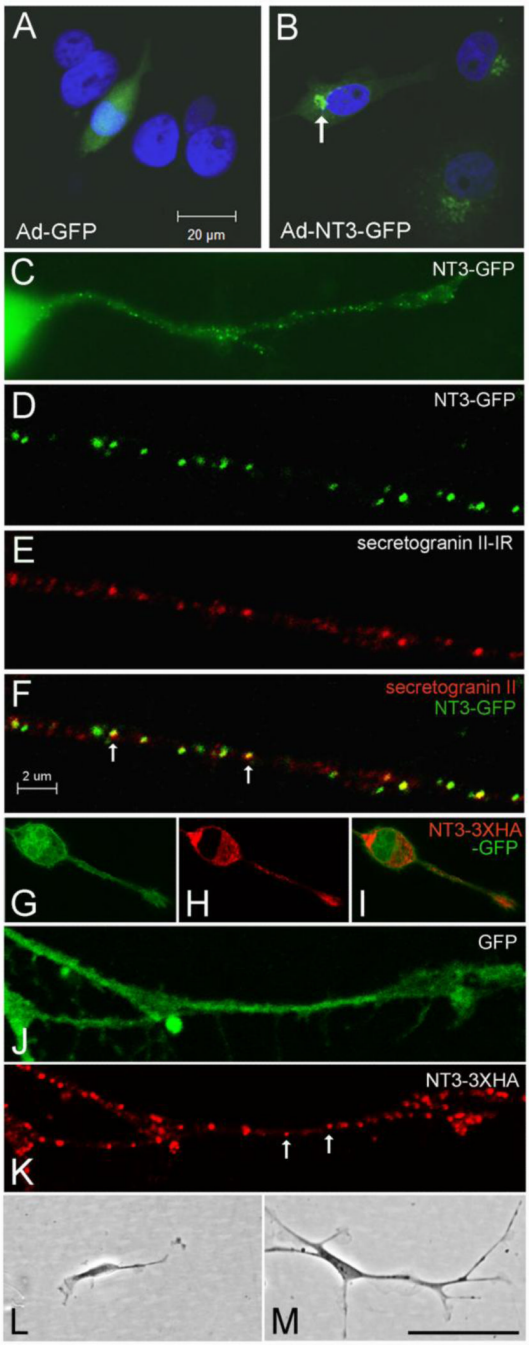

Figure 3.

In vitro localization and bioactivity of NT3 fusion proteins. (A-B) Localization of GFP in COS cells infected with Ad-GFP (A) or Ad-NT3-GFP (B). The arrow in B indicates the fusion protein concentrated in the Golgi apparatus. (C) N2a cell infected with Ad-NT3-GFP showing punctate distribution of GFP within a neurite. (D-F) Confocal images illustrating co-localization of NT3-GFP with secretogranin II-IR (arrows in F) in a neurite extending from a cultured N2a cell. (G-K) N2a cells infected with NT3-3xHA-IRES-GFP contain GFP throughout (G), and HA-IR concentrated in the secretory apparatus, including a vesicular-like distribution within neurites (arrows in K). (L-M) Comparison of DRG neuron morphology at 4 days after treatment with conditioned medium from COS cells infected

with Ad-GFP (L) or with Ad-NT3-3xHA-IRES-GFP (M). Bar in A= 20 μm for A-B. Bar in F= 2 μm for D-F, J-K. Bar in M= 20 μm in C, 42 μm in G-I, 100 μm in L-M.

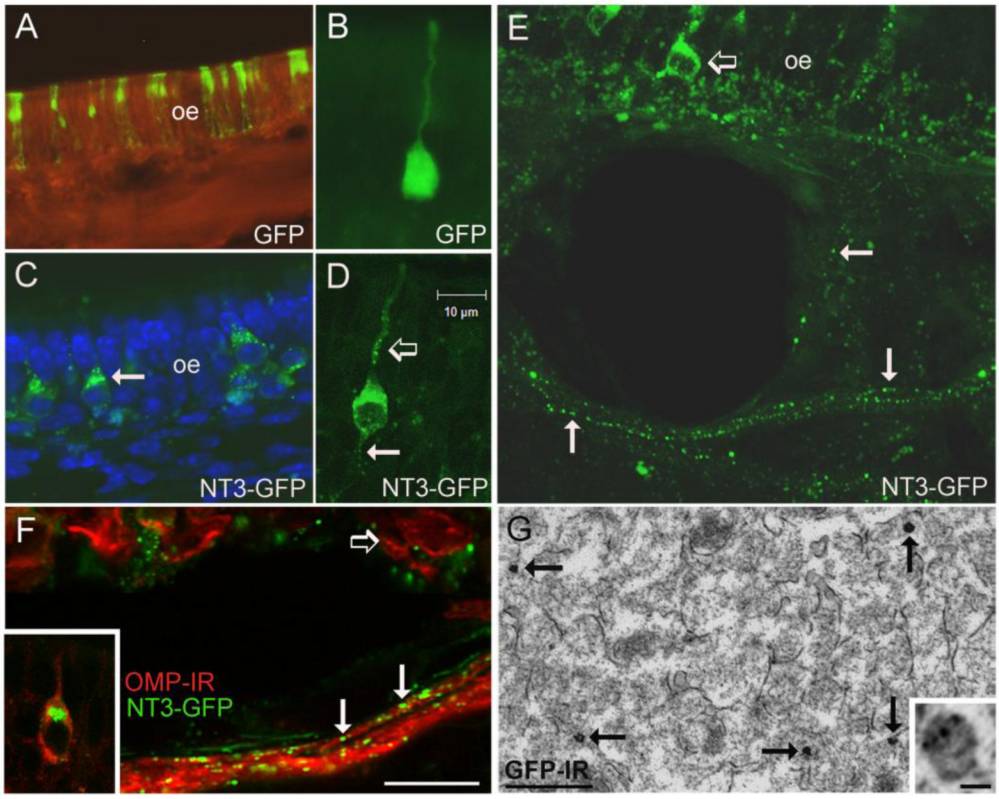

Figure 4.

In vivo infection of olfactory sensory neurons. (A) Expression of GFP in a portion of the olfactory epithelium (oe) at 5 days after irrigation with the Ad-GFP control virus. The GFP label indicates both sensory neurons and sustentacular cells are infected. (B) An olfactory sensory neuron infected with Ad-GFP showing diffuse fluorescence throughout the cell. (C) Distribution of GFP in sensory neurons expressing NT3-GFP. The arrow indicates fluorescence concentrated in the Golgi apparatus. (D) A sensory neuron expressing NT3-GFP at 5 days after infection. Note the punctate distribution of GFP in the dendrite (open arrow) and in the proximal axon segment (arrow). (E) The vesicular-like distribution of NT3-GFP (arrows) can be followed in sensory axons exiting the epithelium. The open arrow indicates a GFP+ sensory neuron. (F) NT3-GFP+ puncta (arrows) are associated with olfactory sensory axons immunoreactive for OMP (red). The open arrow indicates OMP+ neurons in the epithelium, and the inset illustrates NT3-GFP concentrated in the Golgi apparatus of a mature, OMP+ sensory neuron. (G) Electron micrograph showing the distribution of GFP-immunogold-silver labeling in sensory axons in the olfactory nerve layer of a mouse treated with Ad-NT3-GFP. The arrows indicate dense gold-silver deposits, and the inset shows smaller deposits associated with a presumptive secretory vesicle that is less heavily labeled. Bar F= 58μm in A, 15μm in C, 20μm in E, 10μm in F. Bar in D=10μm in B and D. Bar in G= 500nm, inset=40nm.

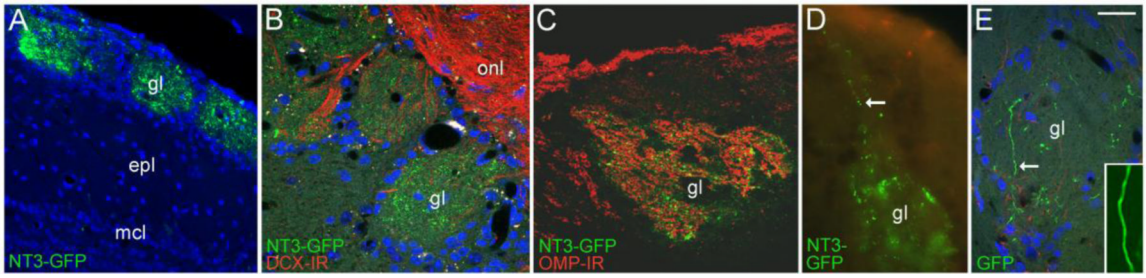

Figure 5.

Anterograde transport of NT3-GFP to the olfactory bulb. (A) NT3-GFP is distributed in bulb glomeruli (gl) at 5 days after sensory neuron infection. (B) Higher magnification image of glomeruli showing the punctate nature of the NT3-GFP label. The section is immunostained with doublecortin antibody to show the overlying olfactory nerve layer (onl). (C) The distribution of NT3-GFP and axonal OMP-IR overlaps within individual glomeruli. (D) Ad-NT3-GFP infected OSNs project axons containing vesicular-like GFP (arrow) to bulb glomeruli. (E) In contrast, neurons infected with control Ad-GFP project axons in which the GFP signal is distributed uniformly (inset). Epl, external plexiform layer; mcl, mitral cell layer. Bar in F= 35μm in A, 23μm in B-C, 14μm in D, 30μm in E, 7μm in inset.

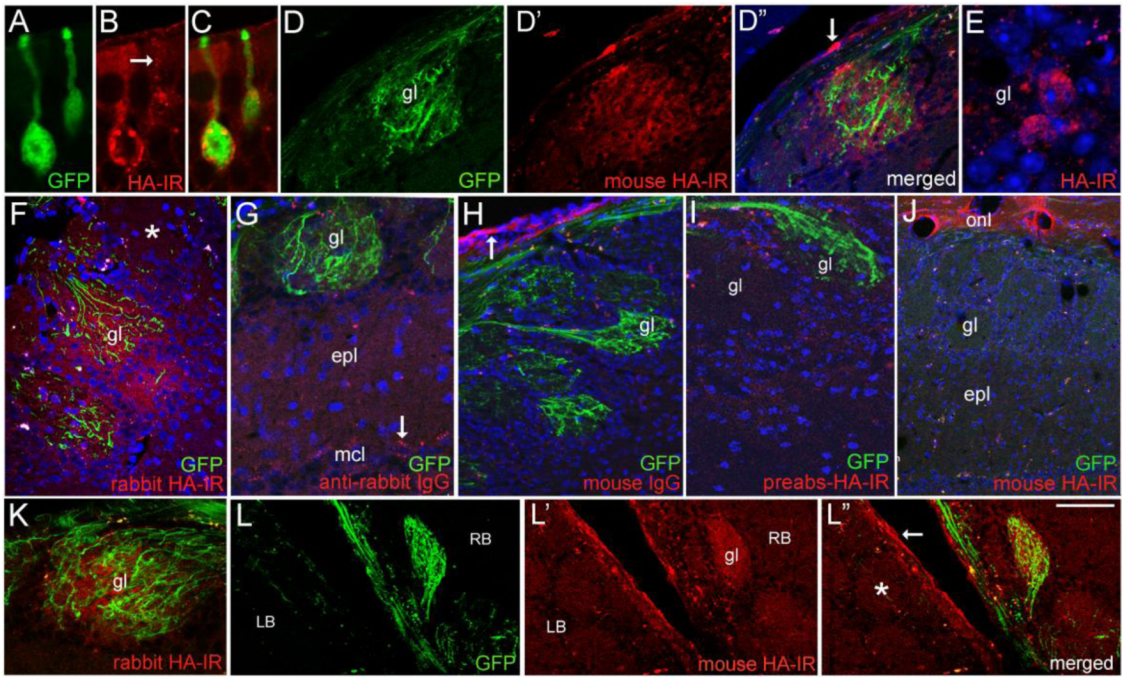

Figure 6.

Expression and distribution of NT3-3xHA in vivo. (A-C) Confocal images comparing the distribution of GFP and mouse HA-IR in sensory neurons 5 days post-infection (d.p.i.) with Ad-NT3-3xHA-IRES-GFP. Vesicular-like distribution of HA is seen in the dendrite (arrow). (D-D") HA-IR is detected in a glomerulus (gl) containing GFP+ axons. The arrow in D" indicates non-specific labeling of ensheathing glia in the outer bulb nerve layer. (E) HA-IR in cell bodies bordering a glomerulus. HA-negative cells are present as well. (F) Glomerular staining produced by rabbit anti-HA antibody (Cell Signaling) at 7 d.p.i. The asterisk indicates a nearby glomerulus that lacks both GFP+ fibers and HA-IR. (G-I) Staining controls showing lack of HA-IR in sections processed without the rabbit primary antibody (G), incubated in mouse IgG (H), or treated with preabsorbed mouse anti-HA (I). The arrow in G indicates autofluorescent particles in mitral cells, and the arrow in H indicates non-specific labeling of ensheathing glia and processes by mouse IgG. (J) A section from the mouse shown in D, showing a bulb area lacking GFP+ axons. Glomerular HA-IR is also lacking, but non-specific staining of ensheathing glia processes occurs in the olfactory nerve layer (onl). (K) A GFP+/HA+ glomerulus at 7 d.p.i (6.5μm optical section thickness). (L-L") Low magnification image of a horizontal section showing the medial right (RB) and left bulbs (LB) at 7 d.p.i. A GFP+ glomerulus (gl) in the right bulb is also HA+. GFP and HA-IR are lacking in glomeruli in the left bulb (asterisk). Non-specific staining occurs in the outer nerve layer (arrow in L"). epl, external plexiform layer; mcl, mitral cell layer. Bar in L"= 12μm in A-C and E, 40μm in D-D" and G, 38 μm in F and I, 64 μm in H, 80μm in J and L-L", and 34 μm in K.

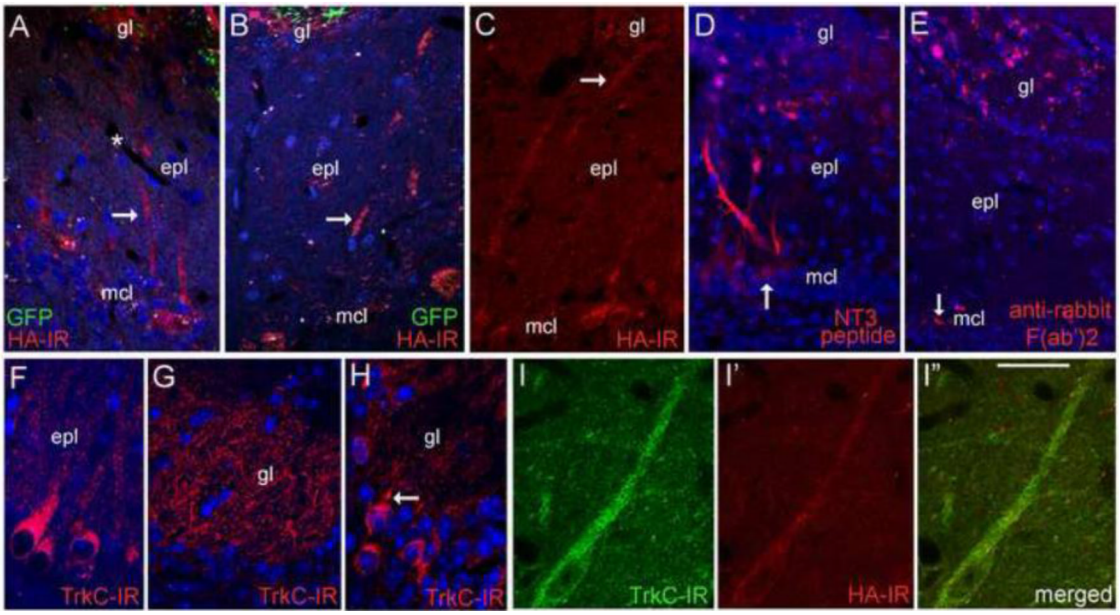

Figure 7.

Bulb neuron accumulation. (A-C) Mitral cells deep to GFP+/HA+ glomeruli exhibit HA-IR. Arrows indicate dendritic processes. The asterisk in A indicates a blood vessel in the external plexiform layer (epl). (D). Labeled bulb neurons are seen 3 hrs after glomerular application of AF568-conjugated NT3 peptide. The arrow indicates a labeled mitral cell body. (E) Mitral cell labeling is not observed after glomerular layer injection of AF568-conjugated F(ab')2 fragments, but fluorescent particles are distributed near the injection site. The arrow indicates autofluorescent particles in the mitral cell layer (mcl). (F-H) TrkC-IR localizes to bulb neurons, including mitral cells and their dendrites (F), dendritic processes within glomeruli (gl, G), and scattered cells located in the glomerular layer (H). The arrow in H indicates a glomerular cell with a proximal dendrite directed toward a glomerulus (I-I") Confocal images showing HA-IR in a TrkC+ tufted cell near a GFP+/HA+ glomerulus at 5 days after intranasal Ad-NT3-3xHA-IRES-GFP treatment. Bar in I" = 46μm in A, 37μm in B, 53μm in C, 56μm in D, 62μm in E, 27μm in F, 21μm in G, and 29μm in H-I".